HHS Public Access

Author manuscript

Nature. Author manuscript; available in PMC 2024 September 06.

Published in final edited form as:

Nature. 2024 March ; 627(8004): 620–627. doi:10.1038/s41586-024-07142-4.

The Hyphal-Specific Toxin Candidalysin Promotes Fungal Gut Commensalism

Shen-Huan Liang[1,#], **Shabnam Sircaik**[1,#], **Joseph Dainis**[1], **Pallavi Kakade**[1], **Swathi Penumutchu**[1], **Liam D. McDonough**[1], **Ying-Han Chen**[2], **Corey Frazer**[1], **Tim B. Schille**[3,6], **Stefanie Allert**[3], **Osama Elshafee**[3], **Maria Hänel**[3], **Selene Mogavero**[3], **Shipra Vaishnava**[1], **Ken Cadwell**[2], **Peter Belenky**[1], **J. Christian Perez**[4], **Bernhard Hube**[3,5,6,*], **Iuliana V. Ene**[7], **Richard J. Bennett**[1,*]

[1]Department of Molecular Microbiology and Immunology, Brown University, Providence, RI 02912

[2]Department of Microbiology, New York University School of Medicine, New York, NY, USA.

[3]Department of Microbial Pathogenicity Mechanisms, Leibniz Institute for Natural Product Research and Infection Biology - Hans Knoell Institute (HKI), Jena, Germany.

[4]Department of Microbiology and Molecular Genetics, McGovern Medical School, The University of Texas Health Science Center at Houston, Houston, Texas, USA.

[5]Institute of Microbiology, Friedrich Schiller University Jena, Germany

[6]Cluster of Excellence Balance of the Microverse, Friedrich Schiller University Jena, Jena, Germany

[7]Institut Pasteur, Université Paris Cité, Fungal Heterogeneity Group, Paris, France.

Abstract

The fungus *Candida albicans* frequently colonizes the human gastrointestinal (GI) tract from which it can disseminate to cause systemic disease. This polymorphic species can transition between growing as single-celled yeast and as multicellular hyphae to adapt to its environment. The current dogma of *C. albicans* commensalism is that the yeast form is optimal for gut

[*]**Correspondence and requests for materials** should be addressed to Richard Bennett or Bernhard Hube. Richard_bennett@brown.edu; Bernhard.Hube@leibniz-hki.de.

[#]These authors contributed equally

Author Contributions

R.J.B. conceived the majority of the experiments and wrote the initial manuscript draft, with input from S-H.L. and S.S. S-H.L. and S.S. performed the majority of the experiments. P.K. performed the microscopic analysis of yeast and hyphal cells. L.M. constructed strains and analyzed *in vivo* phenotypes. J.D. performed analyses of *C. albicans* strains with individual bacterial strains in mice. C.F. assisted with design and construction of *C. albicans* mutant strains. S.V. provided gnotobiotic animals and advised on the project. J.C.P., K.C. and Y-H.C. performed consortia experiments. S. P. and P.B. analyzed 16S data and generated related figures. T.B.S., S.A., M.H., S.M., O.E. performed analyses of *C. albicans* with candidalysin, O.E. performed *in vitro C. albicans* competition experiments, S.A., S.M. performed transcriptional profiling of the *ece1* mutant, B.H. conceived the *in vitro* experiments, provided the *C. albicans ece1* mutant strains and advised on the project. I.V.E. performed *in vivo* experiments and advised on the project.

Competing interests

No competing interests noted.

Additional Information

Peer review information *Nature* thanks the three anonymous reviewers for their contribution to the peer review of this work.

colonization whereas hyphal cells are detrimental to colonization but critical for virulence[1–3]. We reveal that this paradigm does not apply to multi-kingdom communities in which a complex interplay between fungal morphology and bacteria dictates *C. albicans* fitness. Thus, while yeast-locked cells outcompete wildtype cells when gut bacteria are absent or depleted by antibiotics, hyphae-competent wildtype cells outcompete yeast-locked cells in hosts harboring replete bacterial populations. This increased fitness of wildtype cells involves the production of hyphal-specific factors including the toxin candidalysin[4,5], which promotes the establishment of colonization. At later time points, adaptive immunity is engaged, and intestinal immunoglobulin A preferentially selects against hyphal cells[1,6]. Hyphal morphotypes are thus under both positive and negative selective pressures in the gut. Our study further shows that candidalysin has a direct inhibitory effect on bacterial species including limiting their metabolic output. We therefore propose that *C. albicans* has evolved hyphal-specific factors including candidalysin to better compete with bacterial species in the intestinal niche.

Fungi are life-long components of the human microbiota and are acquired soon after birth[7]. Despite being minor constituents of the intestinal microbiota, commensal fungi play key roles in stimulating both local and systemic immune responses. These eukaryotic species can serve protective or pathologic functions, with the latter including roles in inflammatory bowel disease (IBD) and allergenic reactions[5,8–15]. *Candida* species can also escape the commensal niche and cause life-threatening systemic infections, particularly in the immunocompromised host[16–18].

The most clinically relevant fungal species is *Candida albicans,* which can grow as budding yeast or as filamentous hyphae or pseudohyphae[19,20]. This species is a common component of the human gut microbiota and yet the fungal factors promoting commensalism are poorly defined, particularly under homeostatic conditions where fungi are vastly outnumbered by bacteria. Previous studies have established that the yeast-to-hyphal transition is critical for systemic virulence[20–23], and yet yeast-locked forms are optimal for commensalism in germ-free (GF) or antibiotic-treated mice[1–3,24,25]. Indeed, serial passaging of *C. albicans* in the gut of antibiotic-treated mice repeatedly gave rise to yeast-locked forms, establishing that loss of the hyphal state is advantageous in this environment[2].

These observations have led to the paradigm that yeast cells are optimal for gut colonization whereas the hyphal form is detrimental to colonization but critical for disease. However, if filamentation is detrimental to commensal fitness, for what purpose has this program been retained? Indeed, the vast majority of clinical isolates are capable of undergoing the yeast-to-hyphal transition, while a minority are naturally yeast-locked[25]. These observations led us to speculate whether hyphal formation is maintained by certain selective pressures during *C. albicans* colonization of the mammalian host.

Here, we examined *C. albicans* gut colonization in diverse murine models, both in the presence and absence of bacterial competition. We demonstrate that intestinal colonization involves a complex interplay between the morphological state of the fungus and the bacterial microbiome. Thus, yeast-locked cells demonstrate elevated fitness when intestinal bacteria are absent or depleted, whereas hyphae formation is critical for gut colonization when commensal bacteria are prevalent. We show that filamentation is advantageous

for colonization due to the production of hyphal-specific factors including the toxin candidalysin - the first true virulence factor identified in a human fungal pathogen[4,26,27]. Hyphal growth therefore enables *C. albicans* to propagate in bacterially-colonized hosts, establishing that fungal 'virulence factors' act as 'commensalism factors' during inter-kingdom competition in the intestinal niche.

Colonization properties of yeast-locked *C. albicans* cells

We performed a series of competition assays to compare the fitness of wild type (WT) *C. albicans* cells with those lacking the Efg1 transcription factor that are yeast-locked under most conditions[22,28–30]. Previous studies have often utilized antibiotics to promote stable gut colonization with *C. albicans*[1–3,24,25,31]. Here, colonization was compared in hosts fed a standard diet (SD; FormuLab 5001) versus those fed a low-fiber, high-sucrose purified diet (PD; AIN-93G), both with and without antibiotics. PD-fed hosts were previously shown to support long-term *C. albicans* colonization even without antibiotic dysbiosis[32].

We first compared the relative colonization fitness of the standard *C. albicans* WT strain SC5314 with *efg1Δ/Δ* cells constructed in this background. Consistent with previous studies[1–3,24,33], *efg1Δ/Δ* cells outcompeted WT SC5314 cells in mice on antibiotics (penicillin/streptomycin), reaching >90% of the fecal population by two days' post-infection (dpi) independent of whether mice were on the SD or PD (Fig. 1a–c). *efg1Δ/Δ* cells also dominated in gastrointestinal (GI) organs taken from these hosts (Extended Data Fig. 1a,b). In contrast to colonization of antibiotic-treated hosts, however, *efg1Δ/Δ* cells exhibited a striking fitness defect relative to WT SC5314 cells in both SD- and PD-fed mice in the absence of antibiotics (Fig. 1d,e). For PD-fed hosts, WT SC5314 cells made up 96% of the population recovered from fecal pellets by day 3 and 100% of the population by day 7 (Fig. 1e) and dominated in GI organs recovered at the experimental endpoint (Extended Data Fig. 1c). WT cells also dominated in SD-fed hosts, showing significantly higher fitness than *efg1Δ/Δ* cells (Fig. 1d). *C. albicans* WT SC5314 cells show limited colonization of SD-fed hosts without antibiotics (see below) and WT vs. *efg1Δ/Δ* fitness was therefore also compared using *C. albicans* isolates 529L and CHN1 which stably colonize SD-fed mice even without antibiotics[34]. WT versions of both 529L and CHN1 outcompeted *efg1Δ/Δ* derivatives in antibiotic-naïve SD-fed mice and colonization levels were stably maintained in contrast to the outcome observed with SC5314 cells (Extended Data Fig. 1d–f).

The colonization properties of SC5314 WT and *efg1Δ/Δ* strains were further compared by individually inoculating these strains into mice alongside an SC5314 strain lacking *NRG1* that is constitutively filamentous[35–37]. Both *efg1Δ/Δ* and *nrg1Δ/Δ* cells were defective for colonization of PD-fed mice (Fig. 1f), in line with a study showing that hyphal-locked cells are also defective in colonizing antibiotic-treated mice[38]. WT SC5314 cells adopted both yeast and hyphal morphologies in antibiotic-treated hosts, whereas *efg1Δ/Δ* cells were >98% yeast cells and *nrg1Δ/Δ* cells were >90% filamentous cells (Fig. 1g,h). Fungal morphotypes were also evaluated in cecal contents from antibiotic-naïve, PD-fed animals which again showed that WT SC5314 cells adopted both yeast and hyphal forms, whereas *efg1Δ/Δ* and *nrg1Δ/Δ* cells were essentially yeast-locked and hyphal-locked, respectively (Fig. 1i,j).

The fitness of yeast-locked *flo8Δ/Δ* cells was evaluated as *FLO8* is a second transcription factor essential for hyphal development[2] (Extended Data Fig. 2a,b). SC5314 *flo8Δ/Δ* cells outcompeted their WT counterparts in GF and antibiotic-treated hosts (Extended Data Fig. 2c–e) but, like *efg1Δ/Δ* cells, showed decreased relative fitness in antibiotic-naïve PD- and SD- fed mice (Extended Data Fig. 2f,g). Deletion of *FLO8* in strains 529L and CHN1 also resulted in reduced fitness relative to their WT controls in antibiotic-naïve hosts (Extended Data Fig. 2h,i).

Together, these results reveal that yeast-locked cells exhibit a colonization fitness advantage over filamentation-competent WT cells in antibiotic-treated mice that are depleted for bacteria. In contrast, the relative fitness of these strains is reversed in antibiotic-naïve mice where WT cells outcompete yeast-locked (and hyphal-locked) mutants. Both fungal morphotypes (or transitions between morphotypes) are therefore required for GI colonization of antibiotic-naïve hosts. Moreover, these results were independent of the murine diet, fungal strain or mouse background, establishing the generality of these findings.

Antibiotics, diet and *C. albicans* impact bacterial populations

Given that a change in diet or antibiotics can alter fungal gut commensalism, we examined the impact of each of these factors on the bacterial microbiome, both with and without *C. albicans* colonization. In the absence of antibiotics, SD-fed mice displayed decreasing levels of *C. albicans* in the gut and most lost fungal colonization by day 21, whereas PD-fed mice and those on antibiotics exhibited stable *C. albicans* colonization throughout the experiment (Extended Data Fig. 3a,b). SD- and PD-fed mice both showed average bacterial loads of 10^{10}-10^{11} CFUs/g in fecal pellets that decreased 10^{3}-10^{5}-fold upon antibiotic supplementation (Extended Data Fig. 3c,d). Under these conditions, antibiotic-naïve mice therefore harbor an ‘intact’ bacterial microbiota with $>10^{9}$ bacterial CFUs/g. Notably, *C. albicans* colonization did not significantly impact total gut bacterial loads in any of the groups tested (Extended Data Fig. 3c,d).

To assess intestinal bacterial communities, 16S rRNA sequencing was performed. A shift in diet had the largest effect on 16S composition (Extended Data Fig. 3e), with a significantly lower Shannon Diversity in PD-fed mice than in SD-fed mice at days 7 and 10 (Extended Data Fig. 3f). PD-fed mice also harbored higher Deferribacterota (day 1, 3, 14, 21, SI), Proteobacteria (day 10) and Verrucomicrobia (SI), but lower Bacteroidota (day 0, 3) than SD-fed mice (Extended Data Fig. 3g). While species-level analysis from 16S data is challenging, SD-fed mice were initially associated with more Firmicutes, including Bacilli and Clostridia, as well as increased Mycoplasmota (Anaeroplasma), while PD-fed mice were associated with more Alphaproteobacteria (Rhodospirales)(Extended Data Fig. 4a–d). In addition to depleting intestinal bacterial levels, antibiotic treatment shifted the composition of the bacterial microbiome, with a larger effect in PD-fed than SD-fed mice (Extended Data Fig. 3h,i). The most significant effects of antibiotics included an increase in Proteobacteria and Actinobacteria (multiple time points with both diets), as well as a decrease in Bacteroidota at early time points (Extended Data Fig. 3h,i).

C. albicans colonization did not affect overall bacterial levels or alter Shannon Diversity but still had a significant impact on microbiome composition (Extended Data Fig. 3c–d, j–m, Extended Data Fig. 5a–c). *C. albicans* decreased Actinobacteria in PD-fed mice (day 7, 21) and in SD-fed mice given antibiotics (day 3, 21, Extended Data Fig. 3k,m). Eggerthellaceae was the major family represented in the Actinobacteria phylum and the relative abundance of this phylum decreased in several groups that harbored *C. albicans* at day 21 (Extended Data Fig. 3n). *C. albicans* also impacted the Verrucomicrobia phylum; it decreased this phylum in SD-fed mice (day 1, 14, 21) and PD-fed mice with antibiotics (day 10) yet increased this phylum in PD-fed mice without antibiotics (day 7) (Extended Data Fig. 3j–l). At the genus level, *C. albicans* colonization in PD-fed mice led to decreased abundance of Enterorhabdus and Gordonibacter from the Actinobacteria phylum (Extended Data Fig. 4e–h).

Together, these data demonstrate that antibiotic treatment or changing of the diet (from SD to PD) caused substantial changes to gut bacterial populations including a higher abundance of aerobic Proteobacteria, a marker of microbiome dysbiosis[39]. Disruption of the bacterial microbiome was therefore associated with increased fungal colonization. In contrast, introduction of *C. albicans* was associated with limited changes to bacterial populations including the restriction and expansion of certain specific phyla.

Bacteria govern the fitness of *C. albicans* morphotypes

To further address how changes in the bacterial microbiome impact fungal fitness, competition experiments were performed in mice that were GF or harbored specific bacterial communities. Consistent with previous studies[24], GF mice were stably colonized by WT SC5314 cells. Moreover, yeast-locked *efg1Δ/Δ* cells showed equal or higher fitness than WT cells in these hosts; *efg1Δ/Δ* cells outcompeted WT cells in GF C57BL/6 and BALB/c mice (Fig. 2a,b, Extended Data Fig. 6a,b), whereas these cell types showed equivalent fitness in GF NMRI mice (Extended Data Fig. 6c).

To evaluate the effect of different bacterial species on *C. albicans* colonization, WT and *efg1Δ/Δ* cells were inoculated into gnotobiotic mice harboring the Oligo-Mouse-Microbiota of twelve (Oligo-OMM^{12}) or fifteen (Oligo-OMM^{15}) defined bacterial species, or the altered Schaedler flora (ASF) of eight species[40,41]. These consortia, to varying degrees, can limit colonization by enteric pathogens such as *Salmonella enterica* serovar Typhimurium[40]. *C. albicans* competitions revealed that in contrast to GF mice, WT cells rapidly outcompeted *efg1Δ/Δ* cells in the presence of each of the three bacterial consortia (Fig. 2c–e). For example, WT cells represented >99% of the colonizing population by day 7 in mice carrying either the OMM^{15} or ASF consortium (Fig. 2d,e). The presence of each of these defined bacterial populations therefore strongly selects for filamentation-competent WT cells over yeast-locked *efg1Δ/Δ* cells. Total *Candida* colonization levels were also two to three orders of magnitude lower in hosts harboring OMM^{12} or OMM^{15} than in comparable GF hosts (Extended Data Fig. 6e,f).

Similar competitions were performed in ampicillin (Amp)-treated SD-fed mice into which an Amp-resistant (Amp^{R}) Gram-negative or Gram-positive strain had been introduced prior

to *C. albicans* inoculation (Fig. 2f). Amp treatment led to a decrease of three orders of magnitude in gut bacterial loads consistent with previous studies[42], while Amp^R *Escherichia coli*, *Klebsiella pneumoniae* or *Entercoccus faecium* colonized to high levels in Amp-treated mice (Fig. 2g,h). The presence of Amp^R bacteria restricted, but did not prevent, fungal colonization; fungal CFUs were $>10^7$ cells/g in fecal material from Amp-treated mice but decreased to $1.5–4.0 \times 10^6$ cells/g when mice were pre-colonized with Amp^R bacteria (7 dpi; Fig. 2i). Yeast-locked *efg1Δ/Δ* cells outcompeted WT *C. albicans* cells in Amp-treated mice as expected (Fig. 2j), yet inclusion of any of the three Amp^R bacterial species resulted in WT cells rapidly outcompeting *efg1Δ/Δ* cells (population >90% WT by day 5; Fig. 2k–m). Indeed, introduction of *E. coli* cells into a GF host also strongly selected for WT cells over *efg1Δ/Δ* cells (Extended Data Fig. 6d), establishing that bacterial monocolonization is sufficient, at high CFU levels, to drive the selection for filamentation-competent WT cells over yeast-locked cells. In contrast, gavage of heat-killed (HK) *E. coli* cells did not select for WT cells over *efg1Δ/Δ* cells (Extended Data Fig. 6g) indicating that dead bacteria do not impact fungal fitness the same as live bacteria.

Role of adaptive immunity in *C. albicans* colonization

Recent studies have shown *C. albicans* morphotypes are differentially targeted by adaptive immunity in the gut. Hyphal cells preferentially induce intestinal immunoglobulin A (IgA) which binds to prominent hyphal-specific factors including Als1, Als3 and Hwp1[1,6]. Loss of IgA increases the proportion of hyphae present in the gut indicating that the filamentous state is suppressed by antibody responses. This, in turn, can promote the long-term fitness of *C. albicans* populations in GF animals by favoring colonization by yeast-form cells[1,6,43].

Induction of IgA takes at least a week[1] and therefore *C. albicans*-specific IgA did not contribute to the fitness advantages of WT over yeast-locked cells described here, as these arise early (within 1–3 days) following inoculation (Fig. 1e). To further address this point, the fitness of WT and *efg1Δ/Δ* cells was compared between WT and $Rag1^{-/-}$ mice, as the latter lack B- and T-cells. We observed that *C. albicans* WT cells rapidly outcompeted *efg1Δ/Δ* cells in both control and $Rag1^{-/-}$ SD-fed mice without antibiotics (Extended Data Fig. 6h,i), establishing that the increased fitness of WT over yeast-locked *C. albicans* cells is independent of IgA responses at early stages of colonization. Interestingly, overall fungal colonization levels were similar between control and $Rag1^{-/-}$ mice out to 7–10 days yet by 14 days fungal loads were significantly higher in $Rag1^{-/-}$ mice (Extended Data Fig. 6j), consistent with IgA targeting WT *C. albicans* cells at the later time points[1,6].

These results establish that hyphae-competent *C. albicans* cells exhibit an early fitness advantage over yeast-locked cells in mice with an intact (antibiotic-naïve) bacterial microbiome and that this advantage is present in both control and $Rag1^{-/-}$ mice. At later time points, however, adaptive immunity can potentially restrict the fitness of WT *C. albicans* cells, in line with IgA targeting of hyphal-specific cell surface adhesins[1,6].

Hyphal-specific effectors promote gut colonization

We tested whether the increased colonization fitness of *C. albicans* WT cells over yeast-locked forms was due to the expression of specific hyphal-specific genes (HSGs)[20]. HSGs are highly expressed in the gut where their expression is lost upon deletion of *EFG1*[3]. Prominent HSGs include established virulence factor genes such as *ECE1* which encodes the peptide toxin candidalysin[4,26,27,44,45]. This factor damages epithelial cells and has been linked to IBD in patients[5] and to colonization fitness in antibiotic-treated mice[46]. Other prominent HSGs include *ALS3* encoding an adhesin[47] and invasin[48] that mediates iron acquisition[49], and *SOD5* that encodes a superoxide dismutase protective against oxidative stress[50,51].

Each of these HSGs were deleted from SC5314 and their colonization fitness compared to WT controls. Strikingly, loss of either *ECE1* or *ALS3,* but not *SOD5,* resulted in a fitness defect in antibiotic-naïve hosts (Fig. 3a,b; Extended Data Fig. 7a,b,d). For example, competition of WT and *ece1Δ/Δ* cells showed that the colonizing population consisted entirely of WT cells in fecal pellets as early as 7 dpi in PD-fed hosts (Fig. 3b) as well as in GI organs from these mice (Extended Data Fig. 8a,b). A similar colonization defect was observed with *ece1Δ/Δ* cells constructed in the 529L and CHN1 strain backgrounds in antibiotic-naïve hosts (Extended Data Fig. 8c,d). In contrast, loss of *ECE1* (as with loss of *EFG1*) did not substantially decrease fitness in antibiotic-treated or GF mice (Fig. 3c,d, Extended Data Fig. 8e,f), whereas loss of *ALS3* caused fitness defects in both antibiotic-treated and -naïve hosts (Extended Data Fig. 7d,e). The fitness advantage of WT over *ece1Δ/Δ* cells was restored in GF mice by pre-colonization with *E. coli* (Fig. 3e, Extended Data Fig. 8g). These results indicate that bacterial colonization levels determine the relative fitness of WT vs. *ece1Δ/Δ* populations in the gut, as they do for WT vs. *efg1Δ/Δ* cells.

The *ECE1* gene product is proteolytically processed into eight peptides of which the third peptide (pIII) represents the candidalysin toxin. WT cells were competed against *ece1Δ/Δ*+*ECE1*ΔpIII cells that lack only the toxin-encoding peptide and, similar to full *ECE1* gene deletions, *ECE1*ΔpIII cells showed equivalent fitness levels to WT cells in GF mice (Fig. 3f, Extended Data Fig. 8h), but were rapidly outcompeted by WT cells in conventionally-housed antibiotic-naïve mice (Fig. 3g, Extended Data Fig. 8i). Mice were also individually colonized with WT, *ece1Δ/Δ* or *ece1Δ/Δ+ECE1*ΔpIII strains, both with and without antibiotic supplementation. Each of these strains colonized to similar levels in mice on antibiotics (Fig. 3h), in contrast to a previous analysis of *ece1Δ/Δ* cells[46]. WT and *ece1Δ/Δ* cells also showed similar filamentation profiles in these hosts (Fig. 3j,k), consistent with *in vitro* studies[4]. However, *ece1Δ/Δ* and *ece1Δ/Δ*+*ECE1*ΔpIII cells both showed substantial colonization defects relative to the WT strain in antibiotic-naïve mice (CFU levels 26-to-32-fold lower than WT; Fig. 3i). Filamentation of *ece1Δ/Δ* cells was also similar to WT cells when evaluated in cecal contents from these mice (Fig. 3l,m). These results establish that the hyphal program promotes *C. albicans* commensalism in mice harboring an intact bacterial microbiome and does so, at least in part, due to the expression of HSGs such as *ECE1.*

Candidalysin toxin exhibits anti-bacterial properties

To determine how *ECE1* impacts gut commensalism, the global transcriptomes of WT and candidalysin-deficient *ece1Δ/Δ* and *ece1Δ/Δ+ECE1*ΔpIII strains were evaluated. Loss of either the *ECE1* gene or the pIII peptide had little effect on the transcriptome even under filamentation-promoting conditions, including the expression of other HSGs (Extended Data Fig. 9a). WT and *ece1Δ/Δ* cells were engineered to express GFP or RFP to enable *in vitro* head-to-head competitions. Competitions were performed under a variety of biologically relevant conditions including growth in RPMI at 37°C with CO_2, acidic pH (pH 4.7), high salt (1 M NaCl), hypoxia (1% O_2), oxidative stress (2 mM H_2O_2), or in the presence of short-chain fatty acids (2% acetate) (Extended Data Fig. 9b–g). No difference in fitness between WT and mutant was observed in any of these conditions. The ability of *ece1Δ/Δ* and WT cells to grow on epithelial cells also revealed no difference between the two cell types (Extended Data Fig. 9h). WT and candidalysin-deficient cells therefore exhibit similar abilities to propagate under *in vitro* conditions including those associated with physiological stress.

Given that the contribution of Ece1 to commensal fitness depends on bacterial competition, we tested the direct impact of synthetic candidalysin peptide (CaL) on the bacterial species used in our GI colonization assays. Notably, candidalysin peptide significantly reduced the number of CFUs generated by *E. coli*, *K. pneumoniae* and *E. faecium*, resulting in a 2–3-fold decrease in CFU formation by each of these species (Fig. 4a,b). Candidalysin also reduced the metabolic activity of all three bacterial species in a dose-dependent fashion, with 70 μM peptide decreasing *E. coli* metabolism by ~80% (Fig. 4c). Candidalysin decreased glucose consumption in two of the three species (*E. coli* and *K. pneumoniae*) by 1.5-to-2.5-fold (Fig. 4d). Together, these results reveal that candidalysin toxin can directly inhibit the growth and metabolism of commensal bacterial species that compete for resources with *C. albicans* in the gut, in addition to the established role of candidalysin in mediating host cell damage and inflammation.

Discussion

C. albicans is a commensal of the human GI tract where it plays key roles in local and systemic immune responses, in addition to its ability to escape this niche and cause systemic disease. Currently, the yeast form of the species is thought to be optimal for colonization while the filamentous form is deemed detrimental to gut fitness but critical for pathogenesis[1–3,24,33]. From an evolutionary perspective, this raises the question as to why filamentation has been retained by the species if it reduces fitness in the natural environmental niche? Similarly, while candidalysin toxin is an established virulence factor that is essential for epithelial cell damage[4] and associated with escape from macrophages[44], it is unclear what the intrinsic advantage of expressing this toxin provides to commensal fungal cells.

Here, we reveal that both yeast-locked and hyphal-locked *C. albicans* cells are defective in intestinal colonization when an intact (antibiotic-naïve) bacterial microbiome is present. The ability of cells to exist in both morphotypes, or to transition between morphotypes,

is therefore as critical to the commensal fitness of the species as it is for virulence[20–23]. We show that hyphal-specific factors promote initial colonization of the gut due to the expression of HSGs including *ECE1* (encoding candidalysin) and *ALS3* (encoding a multifactorial adhesin and invasion), establishing that these factors provide an intrinsic benefit to the cells producing them.

Fitness differences between WT and yeast-locked cells arise within 1–3 days of inoculation ruling out a role for adaptive immunity in driving this selection, and analysis of colonization in *Rag1*$^{-/-}$ mice further established that such fitness differences are independent of the involvement of adaptive immunity. Notably, WT *C. albicans* colonization levels at later time points (14 days) were higher in *Rag1*$^{-/-}$ mice than in control mice, indicating that adaptive responses restrict fungal colonization and consistent with the observation that mucosal IgA preferentially targets hyphal *C. albicans* cells[1,6]. Hyphal cells are therefore the target of both positive and negative selective pressures in the gut environment.

Our work also establishes that the fitness of different *C. albicans* strains in the gut is determined by bacterial populations in this niche. Most studies of fungal commensalism have utilized antibiotic-treated hosts to promote colonization, yet this dysbiosis alters the relative fitness attributes of WT and mutant *C. albicans* strains. As shown in the current study, yeast-locked cells are hyperfit in mice given antibiotics but exhibit a lower fitness than WT cells in antibiotic-naïve mice where bacterial loads are orders of magnitude higher. Moreover, different bacterial populations can select for WT cells over yeast-locked cells, implicating bacterial colonization levels, rather than specific bacterial species, as responsible for driving this selection.

The impact of *ECE1* on fitness was, like that of yeast-locked cells, most evident in antibiotic-naïve mice harboring high bacterial loads in the gut. Under these conditions, WT cells were fitter than candidalysin-deficient cells during early colonization both when tested individually and in head-to-head competitions. The latter result establishes that toxin production provides an intrinsic benefit to toxin-producing cells rather than a change to the environment that favors all commensal *C. albicans* cells. Loss of *ECE1* did not markedly alter the *C. albicans* transcriptome or fitness *in vitro*, including during infection of epithelial cells. Candidalysin had a direct inhibitory effect, however, on the growth and metabolism of bacterial species shown to compete with *C. albicans in vivo*. These results implicate candidalysin in promoting gut commensalism through the direct targeting of bacteria that are competing for resources with *C. albicans*. This toxin therefore supports the establishment of fungal colonization by mechanisms distinct from, or in addition to, its established roles in cell damage and mucosal inflammation[4,5]. Future studies will further address the specificity of candidalysin on different bacterial species and whether this toxin has additional functions that enable fungal gut colonization.

In summary, we reveal that virulence factors produced by *C. albicans* hyphal cells are also *bona fide* commensalism factors that support fungal propagation in the gut when bacterial competition is high. These factors provide intrinsic benefits to the fitness of fungal cells, consistent with commensal niches acting as ‘training grounds’ for the selection of traits that are critical to both commensalism and pathogenicity[52].

Methods

Mice

Age- and gender-matched mice were used in this study. Animals were monitored under care of full-time staff, given access to food and water ad libitum and maintained under a 12-h light/dark cycle, with temperature maintained at 22–25°C and a relative humidity of 30–70%. Unless stated otherwise, conventional WT 7- to 8-week-old, female BALB/c mice (strain code 028) and 7- to 8-week-old, female C57BL/6J mice (stock# 000664) were obtained from Charles River Laboratories and The Jackson Laboratory, respectively, to perform experiments at Brown University. Male and female GF BALB/c mice (4–5 weeks old) obtained from Taconic Biosciences (Extended Data Fig. 2b, 6b) and female GF WT C57BL6 (9–10 weeks old) from the National Gnotobiotic Rodent Resource Center (NGRRC) (UNC, Chapel Hill, NC) were housed and conducted experiments in a flexible isolator bubble at Brown University (Fig. 3d,f and Extended Data Fig. 8d,e). NMRI mice were bred and raised under germ-free conditions in the Central Animal Facility of the Hannover Medical School (Hanover, Germany) (Extended Data Fig. 6c,d). Mice of both sexes 7–10 weeks of age were employed. Littermates of the same sex were randomly assigned to experimental groups. After inoculation with *C. albicans*, mice were maintained in ventilated cages. Female GF C57BL6 mice (7–8 weeks old) at the New York University (NYU) Grossman School of Medicine Gnotobiotics Animal Facility were used to conduct the experiments in Bioexclusion cages (Tecniplast) (Fig. 2b,c). Male altered Schaedler flora (ASF)[53] C57BL6 mice (6 weeks old) from Taconic Biosciences were used to perform the animal study in Taconic's Isolator Breeding Solutions (IBS) facility housed in a gnotobiotic study isolator (Fig. 2e). Female GF C57BL/6J mice (11–12 weeks old) from NGRRC were used for experiments performed at University of North Carolina (UNC) (Fig. 3e and Extended Data Fig. 8e). Mice were assigned randomly to experimental groups and colonization assays were performed unblinded to know the identity of each group.

Media and reagents

Yeast extract peptone dextrose (YPD) and synthetic complete dextrose (SCD) medium were made as previously described[54,55]. YPD containing 200 μg ml^{-1} nourseothricin (Jena Biosciences, Germany) was used to select nourseothricin-resistant (NAT^R) strains. SC+maltose plates were prepared as synthetic complete dextrose (SCD) but with 2% maltose instead of 2% dextrose. *E. coli* and *K. pneumoniae* were grown and maintained in Luria broth (LB) while *E. faecium* was grown in Todd Hewitt Broth (THB).

Construction of plasmids and *C. albicans* strains

Oligonucleotides and *C. albicans* strains used in the present study are listed in Supplementary Tables 1 and 2, respectively. To create the *efg1Δ/Δ* strain, pRB721[33] was linearized with *Apa*I and *Sac*I and transformed into SC5314, 529L or CHN1 to generate *efg1Δ/EFG1* derivatives. Integration was checked by PCR with oligos 2284/4438 and 2286/4439 for 5' and 3' junctions, respectively. The *SAT1* marker was recycled after growing on SC+maltose medium and the second allele of *EFG1* was deleted in SC5314 and CHN1 backgrounds by transformation with linearized pRB721 to generate *efg1Δ/Δ* strains. PCR with oligos 819/828, 2284/4438 and 2286/4439 was used to check ORF,

5’ junction and 3’ junction, respectively. Mutant strains were grown on SC+maltose to recycle the *SAT1* marker, resulting in nourseothricin-sensitive (NAT^S) *efg1Δ/Δ* strains (CAY10195 and CAY10965 in SC5314, and CAY11184 in CHN1). To delete the second *EFG1* allele in 529L, PCR with oligos 5948/5949 was used to amplify a hygromycin B (HYG) resistance cassette from pRB195[56] and transformed into *efg1Δ/EFG1* to generate *efg1Δ/Δ* (CAY11482). PCR using oligos 819/828, 4476/1458 and 2910/1459 was used to check ORF, 5’ junction and 3’ junction, respectively.

To delete *FLO8*, a *pSFS-FLO8* KO plasmid (pRB989) was generated by PCR amplifying the *FLO8* 5’ and 3’ flanking regions using oligos 4988/4989 and 4990/4991, respectively, and inserting into *Apa*I/*Xho*I and *Sac*I/*Sac*II sites in pSFS2A[57]. pRB989 was linearized by *Apa*I and *Sac*I and transformed into WT 529L and CHN1 cells to generate *flo8Δ/FLO8* cells. PCR with oligos 4982/2274 and 5076/739 was used to check cassette integration. After recycling the *SAT1* marker by growing on SC+maltose medium, linearized pRB989 was again used to delete the second *FLO8* allele to generate *flo8Δ/Δ*. PCRs were performed to check the ORF, 5’ junction and 3’ junction using oligos 4986/5200, 4982/2274 and 5076/739, respectively. Cells were grown on SC+maltose medium to produce NAT^s *flo8Δ/Δ* mutants in 529L (CAY11180) and CHN1 (CAY11186).

To generate SC5314 *ece1Δ/Δ* (CAY8785), oligos 4248/4249 were used to PCR amplify the *ARG4* and *HIS1* cassettes from CAY8578 (*ece1Δ/Δ*[4]) and transformed into strain SN95[58]. Cells were grown on SC medium without arginine to select transformants. Junction PCR checks were performed using oligos 4252/4287 and 4286/4253. The transformation was repeated to delete the second *ECE1* allele and transformants grown on SC medium lacking histidine and arginine. Transformants were PCR checked using oligos 4250/4251 for ORF, 4252/4289 for the 5’ junction and 4288/4253 for the 3’ junction.

To delete *ECE1* in 529L and CHN1, a *pSFS-ECE1* KO plasmid (pRB1481) was generated by inserting the 5’ and 3’ flanking regions of *ECE1*, PCR amplified using oligos 6207/6208 and 6205/6206, into *Sac*I/*Sac*II and *Kpn*I/*Xho*I sites in pSFS2A[57]. pRB1481 was linearized by *Kpn*I/*Sac*I and transformed into 529L and CHN1. Cassette integration was examined by PCR using oligos 4438/4248 and 4439/6277. The *SAT1* marker was recycled, and the transformation was repeated to delete the second *ECE1* copy. The 5’ junction, 3’ junction and ORF were analyzed by PCR using oligos 4438/4248, 4439/6277 and 201/2810, respectively. The resulting strain was grown on medium containing maltose to recycle the *SAT1* marker resulting in a NAT^S *ece1Δ/Δ* mutant in 529L and CHN1 strain backgrounds (CAY12441 and CAY12446, respectively).

To create an isogenic prototrophic wildtype SC5314 strain, *HIS1* and *ARG4* genes were integrated into strain SN95[58]. PCR with oligos 4114/4115 was used to amplify *HIS1* from SC5314 and the amplicon was transformed into SN95, with selection on SC medium without histidine. Cassette integration was checked by PCR using oligos 2623/4289 and 2624/4288. The *ARG4* gene was integrated using the plasmid pEM003[59] digested with *Mfe*I/*Sac*I, and transformants selected on SC medium lacking histidine and arginine. Integration was PCR checked using oligos 6044/6045 and 6046/6047.

To generate NAT^R strains, the pDis3 plasmid was used to integrate into the *NEUT5L* locus as described previously[60]. The plasmid was linearized by *Ngo*MIV and transformed into SC5314 *efg1Δ/Δ* (CAY10195), *flo8Δ/Δ* (yLM794[61]) and *ece1Δ/Δ* (CAY8785) to create NAT^R versions CAY11750, CAY9796 and CAY11507, respectively. PCR checks were performed using oligos 3055/3056.

To delete *SOD5*, plasmids were constructed where the *HIS1* and *LEU2* markers were flanked by 500 bp of homology from *SOD5*. The *sod5::HIS1* plasmid (pRB2151) was constructed via Golden Gate Assembly using *Bsm*BI. A 500 bp fragment from upstream of *SOD5* was amplified from SC5314 using oligos 8551/8552. *HIS1* was PCR amplified from pSN52[58] in two parts to mutagenize an endogenous *Bsm*BI site. The 5' and 3' regions of *HIS1* were PCR amplified with oligos 7006/7007 and 7008/7009, respectively. A 500 bp fragment downstream of the *SOD5* ORF was PCR amplified from gDNA with oligos 8553/8554. These four fragments were assembled into pGGASelect (NEB). The *sod5::LEU2* plasmid (pRB2153) was constructed using the same upstream and downstream 500 bp fragments, combined with the *LEU2* marker amplified from pSN40[58]. The KO cassette from pRB2151 was released by digestion with *Pac*I and transformed into SN87[58] to create *sod5*::*HIS1*/*SOD5* strains CAY14705/14706. Integration was PCR checked using oligos 7510/7834 and 8596/8558. The second *SOD5* allele was disrupted with *LEU2* using *Pac*I-digested pRB2153 and junction checked by PCR using oligos 7510/5056.

Murine GI infection

Murine GI infections by oral gavage were performed as previously described[25]. *C. albicans* cells were cultured in YPD medium overnight at 30°C. The overnight cultures were diluted 50-fold into fresh YPD medium and grown for 4 h at 30°C. Cells were washed with sterile water three times. To perform *C. albicans* competitions, the inoculum was composed of one NAT^S and one NAT^R isolate at a ratio of 1:1. Mice were orally gavaged with a total of ~10^8 fungal CFUs (counted by hemocytometer) in 0.5 ml of water using plastic feeding tubes (Instech Laboratories) for experiments done at Brown University, NYU and University of Wuerzburg. An inoculum of ~10^8 CFUs in 0.2 ml of water was used to inoculate mice in Taconic Biosciences. For the study performed in UNC, an inoculum of ~5×10^7 CFUs in 0.1 ml of water was used. Due to the difficulty of performing oral gavage with GF mice in gnotobiotic conditions, *C. albicans* was added to the drinking water at a final concentration of ~2×10^6 CFUs ml^{-1}. Inoculum water was replaced with sterile water after 24 h. Two mice were cohoused in each cage. Fecal pellets were harvested at the indicated time points and GI organs (stomach, small intestine, cecum and colon) were collected at the end of the experiment. GI organs were homogenized in PBS with antibiotics (500 μg ml^{-1} penicillin, 500 μg ml^{-1} ampicillin, 250 μg ml^{-1} streptomycin, 225 μg ml^{-1} kanamycin, 125 μg ml^{-1} chloramphenicol, and 25 μg ml^{-1} doxycycline) and cultured on YPD and YPD+NAT media to determine CFUs of NAT^R and NAT^S strains.

Conventional mouse models utilized a standard diet (SD; FormuLab 5001, PMI Nutrition International) or a purified diet (PD; AIN-93G; Dyets, Inc.). When antibiotics were included, they were present in the drinking water (1,500 U ml^{-1} of penicillin, 2 mg ml^{-1} of

streptomycin and 2.5% glucose for taste) for four days prior *to C. albicans* inoculation. Mice remained on the indicated diet with or without antibiotics throughout the experiment.

Colonization experiments with individual *C. albicans* strains were carried out for WT SC5314, *efg1Δ/Δ* and *nrg1Δ/Δ* strains using female Balb/c mice from Charles River Laboratory that were 7–8 weeks of age and that were allowed to acclimate in the animal facility for 4 days. Mice were housed together initially and were fed the PD for one week. Colonization of mice with *C. albicans* strains was performed by gavaging 10^8 fungal CFUs in water.

To perform *C. albicans* competitions with ampicillin-resistant (Amp^R) bacteria (*Klebsiella pneumoniae* B425, *Escherichia coli* B427 or *Enterococcus faecium* B460), ampicillin (Amp) was dosed into the drinking water at the final concentration of 0.5 g L^{-1} for four days prior to bacterial inoculation for conventional mice. Bacterial strains were cultured in LB medium at 37°C overnight. The overnight cultures were washed twice with PBS and resuspended in PBS at half the original volume. To generate the heat-killed (HK) *E. coli* (B427), bacterial cells were heated at 70°C for 30 min. Bacterial cell death was verified by plating the inoculum on LB + carbenicillin (100 μg ml^{-1}). HK *E. coli* were inoculated every other day after the first inoculation throughout the experiment. Inoculation of *C. albicans* cells was performed three days following bacterial inoculation. Mice were housed individually after supplementing ampicillin into the drinking water. Mice were fed a SD and remained on Amp throughout the experiment. CFU of Amp^R bacteria was determined by plating on LB + carbenicillin. Bacterial strains used in this study are listed in Supplementary Table 3.

GF NMRI mice were maintained carrying the Oligo-Mouse-Microbiota (OMM^{12})[40]. OMM^{12} contains 12 bacterial strains including *Acutalibacter muris* KB18, *Flavonifractor plautii* YL31, *Clostridium clostridioforme* YL32, *Blautia coccoides* YL58, *Clostridium innocuum* I46, *Lactobacillus reuteri* I49, *Enterococcus faecalis* KB1, *Bacteroides caecimuris* I48, *Muribaculum intestinale* YL27, *Bifidobacterium longum* subsp. *animalis* YL2, *Turicimonas muris* YL45 and *Akkermansia muciniphila* YL44. The OMM^{15} consortium was previously described[40,62] and contains OMM^{12} plus *Escherichia coli* Mt1B1, *Staphylococcus xylosus* 33ERD13C, and *Streptococcus danieliae* ERD01G.

Male C57BL6 mice carrying the ASF^{53} (consisting of *Parabacteroides goldsteinii* ASF519, *Eubacterium plexicaudatum* ASF492, *Schaedlerella arabinosiphila* ASF502, *Pseudoflavonifractor Sp.* ASF500, *Clostridium sp.* ASF356, *Mucispirillum schaedleri* ASF457, *Ligilactobacillus murinus* ASF 361 and *Lactobacillus intestinalis* ASF360) were inoculated with *C. albicans* cells immediately after transfer from the gnotobiotic breading isolator into a gnotobiotic study isolator in the Taconic IBS facility. Fecal samples were collected at indicated time points and stored in 25% glycerol at −80°C and shipped to Brown University on dry ice where they were processed to determine fungal populations.

Female GF C57BL6 mice were orally inoculated with *E. coli* promptly after transfer out of the gnotobiotic isolator. Mice were inoculated with *C. albicans* three days post *E. coli* inoculation. Fecal samples were collected at indicated time points and stored in PBS buffer

with 25% glycerol at −80°C and shipped to Brown University on dry ice where they were processed to determine the fungal populations.

Analysis of *C. albicans* morphology *in vitro* and *in vivo*

C. albicans morphology was analyzed *in vitro* by overnight culture in YPD at 30°C. From overnight cultures, 10^7 cells were subcultured into 10 mg/ml concentrated and filtered cecal contents collected from PD-fed BALB/c mice for 3 h. Cells were washed twice with PBS and stained with 100 μg/ml Calcofluor White for 15 min. Cells were further washed twice with PBS, resuspended in PBS and imaged using Zeiss Axio Observer microscope.

C. albicans cells in the different GI sections were imaged by immunofluorescence analysis. 1–2 cm pieces of GI tract segments (ileum and colon) were fixed in methacarn (American Master Tech Scientific) immediately after harvesting and stored overnight at 22°C. The following day, fixed tissues were washed twice with 70% ethanol and embedded into paraffin blocks (Leica EG1150C). To evaluate *Candida* morphology in the murine GI tract, 10 μm tissue sections, made by an automated microtome (Leica RM2265), were deparaffinized, blocked with PBS plus 5% FBS for 30 min at 22°C, and incubated with an anti-*Candida* antibody coupled to fluorescein isothiocyanate (FITC) (1:500 dilution; PA173154, Thermo Fisher Scientific) overnight at 4°C. This was followed by three washes with PBS at 22°C and staining of the epithelial nuclei with 4,6-diamidino-2-phenylindole (DAPI, Invitrogen). Cell counting was carried out using a Zeiss Axio Observer Z1 Microscope. Tissue sections from a group of 3–5 mice were stained and 100 to 1200 *Candida* cells per section were assessed for morphology.

16S rRNA Sequencing

Nucleic acids (DNA) were isolated from samples utilizing the ZymoBIOMICS Quick-DNA Fecal/Soil Microbe 96 Kit (Zymo Research, D6011, Irvine, CA, United States) following the manufacturer's guidelines. DNA was eluted in nuclease-free water, and quantification performed using the dsDNA-HS assay on a QubitTM 3.0 fluorometer (Thermo Fisher Scientific, Waltham, MA, United States). The 16S rRNA V4 hypervariable region was amplified from the entire DNA pool by utilizing the barcoded 515F forward primer and the 806R reverse primers, as established by the Earth Microbiome Project[63]. This involved generating amplicons using 5X Phusion High-Fidelity DNA Polymerase: initial denaturation at 98°C for 30 s, succeeded by 25 cycles of 98°C for 10 s, 57°C for 30 s, and 72°C for 30 s, finalized by extension at 72°C for 5 min. Following amplification, samples underwent visualization via gel electrophoresis and were combined in equal proportions. The consolidated amplicon library was analyzed by the Rhode Island Genomics and Sequencing Center at URI (Kingston, RI, United States) using an Illumina MiSeq platform. Sequencing encompassed paired-end sequencing (2 × 250 bp) employing the 600-cycle kit along with established protocols. The raw reads were submitted to the NCBI Sequence Read Archive (SRA) and can be accessed under BioProject PRJNA1008281.

16S rRNA Sequencing Analysis

Raw paired-end FASTQ reads were demultiplexed using idemp (https://github.com/yhwu/idemp/blob/master/idemp.cp). Reads were subjected to quality filtering, trimming, de-

noising with DADA2[64] (via q2-dada2), and merging using the Qiime2 (Quantitative Insights Into Microbial Ecology 2 program) pipeline (version 2021.8)[65]. Ribosomal sequence variants were aligned with mafft[66] (via q2-alignment), and phylogenetic tree construction was done with fasttree2[67] (via q2-phylogeny). Taxonomic assignment was done with the pre-trained Naive Bayes classifier and the q2-feature-classifier[68] trained on the SILVA 132 99% database[69]. Alpha diversity (Shannon, Faith's phylogenetic diversity) and beta diversity (Bray-Curtis dissimilarity)[70,71] were calculated using the phyloseq package (version 1.42.0) in R (version 4.2.3)[72]. Significance was determined by the Benjamini, Krieger and Yekutieli test to correct for False discoveries with adjusted p-value < 0.05[73]. Linear discriminant analysis **(**LDA) analysis was conducted using LEfSe (Linear discriminant analysis Effect Size) (Galaxy Version 1.0, http://huttenhower.sph.harvard.edu/galaxy)[74,75].

Quantitative PCR of fecal bacteria

Quantitative PCR (qPCR) (iTaq Universal SYBR Green Supermix, Bio-Rad) was performed to determine the bacterial loads in fecal pellets using universal 16S rRNA primers (oligo 7212 and 7213) as previously described[31]. Bacterial genomic DNA (gDNA) was purified using a ZymoBIOMICS DNA Miniprep Kit (Zymo Research). Bacterial abundance was determined using standard curves with gDNA from *in vitro E. coli* culture.

Transcriptional profiling

Isolation of RNA was performed as described[76]. Briefly, *C. albicans* cells were harvested from 30°C YPD overnight cultures, washed with PBS and 10^7 yeast cells/ml incubated in petri dishes for 3 h at 37°C 5% CO_2 in RPMI. Hyphal cells were collected by scraping and subsequent centrifugation at 3,000 g for 2 min. RNA was isolated using the RNeasy Minikit (Qiagen) combined with an upstream glass bead disruption protocol. RNA concentration and quality were verified using the NanoDrop 1000 and the Agilent 2100 Bioanalyzer Nanochip system, respectively, according to the manufacturers' instructions. Microarray analyses were performed as described previously[77,78]. Briefly, the one-color QuickAmp labelling kit (Agilent) was used to generate cRNA with fluorescently labelled CTP (Cy5 or Cy3 CTP; GE Healthcare) from high-quality total fungal RNA. Labelled cRNA was purified using the RNeasy Minikit (Qiagen), and sufficient dye incorporation was verified by spectrophotometry with the NanoDrop instrument. *C. albicans* arrays were purchased from Agilent technologies (GEO accession number GPL19932). The Gene Expression Hybridization kit (Agilent) was used according to the manufacturer's instructions, using a two-color hybridisation system. The arrays were hybridized in triplicate for each strain. The arrays were scanned with a GenePix 4200AL scanner (GenePix Pro 6.1; 635 and 594 nm; automatically determined photomultiplier tube [PMT] gains; pixel size 5 nm). Data were extracted using the Agilent Feature Extractor (Version 12.0) and imported into GeneSpring 14.9 (Agilent) for analysis. All microarray data are available at the in ArrayExpress under accession MTAB-13349.

In vitro competition experiments

Assays were conducted between WT and *ece1Δ/Δ* reporter strains under hypoxia, low pH, oxidative stress, osmotic stress, or in the presence of a short-chain fatty acid (sodium acetate

[Sigma-Aldrich]). Strains were grown overnight in 1 % YPD at 30°C and 180 rpm. 500 μl of each strain was washed twice with sterile PBS and re-suspended in the same volume. 1:1 mixtures of the WT and *ece1*Δ/Δ reporter strains were incubated for 24 h in liquid RPMI to a final concentration of 2×10^5 cells/ml in the 12-well plate. After 24 h, the 12-well plate was centrifuged for 10 min at 4000 g and the supernatant was carefully removed. The hyphal aggregates were re-suspended in 1 ml PBS containing 1 mg Zymolyase®20T (Amsbio) and incubated for 3 h at 37 °C. Following Zymolyase treatment, hyphal fragments were transferred to a 1.5 ml microcentrifuge, collected at 10000 xg for 5 min, washed once with PBS, then re-suspended in the same volume. Quantification of the two labeled populations in a mixture was carried out via BD FACSVerseTM flow cytometer [BD Bioscience] equipped with an argon laser emitting at 488 nm. The fluorescence signal of the GFP reporter strains was detected using the FITC-A channel equipped with a 527 nm band-pass filter (bandwidth 15 nm) while the RFP signal was detected using the PerCP-A channel equipped with a 700 nm band-pass filter (bandwidth 54 nm). Gating of single hyphal cells was achieved as follows. First, the fragmented hyphal populations were separated from cell debris and selected via SSC-A (side scatter) and FSC-A (forward scatter) signals. Second, duplet cells were excluded via FSC-W and FSC-H signals. 100,000 events were analyzed per sample at a flow rate of approximately 1000 events/second. Both qualitative and quantitative analyses of the *C. albicans* labeled strains were performed with FlowJo® (Version 10.2) software.

In vitro competition experiments on epithelial cell lines were conducted using TR146 human buccal epithelial cells from ECACC (European Collection of Authenticated Cell Cultures; Sigma-Aldrich, 10032305–1VL). The cells were cultured in DMEM-F12 with 10% FBS at 37°C and 5% CO2. For experiments, TR146 cells were seeded and incubated till confluency. Reporter strains of *C. albicans* from overnight cultures were mixed in equal proportions in DMEM-F12 to a concentration of 1×10^7 cells/ml. Infection mixtures were added to TR146 cells to a final concentration of 2×10^5 *Candida* cells/ml. After 24 h, cells were centrifuged (10 min, 4000xg), washed with PBS, and treated with DNase I (2 μl; 1 U/μl) in DNase I buffer (10 mM Tris-HCl, 2.5 mM $MgCl_2$, 0.5 mM $CaCl_2$; pH 7.6) for 1 h at 37°C. Cells were centrifuged and the supernatant removed. Hyphal aggregates were fragmented using 1 mg/ml Zymolyase®20T (Amsbio) in PBS for 3 h at 37°C. Samples were centrifuged and resuspended in 1 ml PBS and analyzed via flow cytometry as described above (500,000 events analyzed at a flow rate of 2000 events/s). Single reporter strains seeded on TR146 cells and mixed in a 1:1 ratio after 24 h growth was used as controls.

The competitive index (CI) was used to estimate the relative fitness of a single strain in competition assays. To calculate the CI between two competing strains, the following formula was used; (Strain A) Day x competition / (Strain B) Day x competition / (Strain A) Day x single strain / (Strain B) Day x single strain.

In vitro candidalysin assays

Candidalysin (CaL) used in this study was synthetically synthesized corresponding to the processed third peptide of the precursor protein Ece1 of *C. albicans* (SIIGIIMGILGNIPQVIQIIMSIVKAFKGNK)[4]. Peptides were obtained from Peptide

Protein Research Ltd. (Southampton, UK), dissolved in ultra-pure water (MQ water, Merck Millipore) to a concentration of 1.4 mM and stored at −20°C.

Bacterial CFU assays with candidalysin

E. coli, *K. pneumoniae* and *E. faecium* were grown in LB at 37°C at 180 rpm overnight. Stationary phase cultures were washed twice with PBS and set to OD 0.04 in PBS in 1.5 ml tubes. Cell suspensions were incubated for 2 h at 37 °C with shaking. Suspensions were re-diluted to OD_{600}=0.02 with PBS with or without 70 μM of the peptide and incubated at 37 °C with shaking. Every 30 min, cells were removed and plated on LB agar plates and incubated overnight. Analysis was performed in biological triplicates for each bacterial species.

XTT assay

XTT assays were performed to analyze the effect of candidalysin on the metabolic activity of bacteria by adaption of assays from Miramón et al[79]. Stationary phase overnight cultures of bacteria were washed twice with PBS and adjusted to an OD_{600} which equals 10^9 CFU/ml. Candidalysin dilutions were prepared in MQ water. The test conditions contained 50 μL of the respective peptide dilution (final concentration: 20–70 μM), 50 μL of the bacterial suspension and 100 μL DMEM. For controls, peptide dilutions were replaced with MQ water, and the bacteria suspension was replaced by PBS. Plates were incubated at 37°C, 18% O_2 and 5% CO_2. After 200 min, 100 μL of XTT mixture (final 1 mg/mL XTT [Fluka] and 0.1 mg/mL CoQ0 [2,3-dimethoxy-5-methyl-p-benzoquinone] [Sigma]) was added to each well and the plate was incubated for another 60 min. The plate was centrifuged at 250g for 10 min. The supernatant was transferred to a clean 96-well plate and measured in a microplate reader (absorbance 451 nm, absorbance 600 nm for reference). All conditions were done in technical duplicates and the assay was performed at least three times for each of the selected bacteria. The value of the reference measurement and the value of the media control were subtracted from the data. The data of the test conditions was evaluated as a percentage of the normal control.

Glucose consumption assay

Stationary phase overnight cultures of bacteria were washed twice with PBS and adjusted to an OD_{600} which equals 10^9 CFU/ml. The test conditions contained 50 μL of the respective peptide dilution (final concentration: 70 μM), 50 μL of bacterial suspension and 100 μL minimal media (0.67% YNB, 0.2% glucose, 1% casamino acids, 25 mM MES pH 6). For controls, peptide dilutions were replaced with MQ water. The plate was incubated at 37°C, 18% O_2 and 5% CO_2 for 200 min before the plate was centrifuged at 250 ×g for 10 min. The supernatant was diluted in PBS in a clean 96-well plate and measured with the GlucoseGlo™-Kit (Promega) according to the manufacturer's instructions. The background measurement (PBS only) was subtracted from each sample. All conditions were done in technical duplicates and the assay was performed at least three times for each of the selected bacteria.

Statistical Analysis

For significant differences between experimental groups MaAsLin2 (Microbiome Multivariable Association with Linear Models)[80] was used with R version 4.2.3. Effect size calculations were done with PERMANOVA (permutational multivariate ANOVA) with the adonis function in phyloseq version 1.42.0 with R version 4.2.3. For LDA analysis by LEfSe, differentially abundant species with LDA score >2 is shown. Kruskal-Wallis was used to test to compare features between diets ($p<0.05$). Pairwise Wilcoxon to compare between taxa ($p<0.05$). Paired parametric t-tests were used to determine significant differences in the proportion of two *C. albicans* populations in the *in vivo* competition assays. Unpaired nonparametric Mann–Whitney *U*-tests were used to determine the significance between colonization levels of different strains in the monocolonisation assays. Unpaired parametric t-tests were used to determine significant differences in the treated and control samples for in vitro bacterial CFU assays, XTT assays and glucose consumption assays. *P* values for all t-tests were calculated using GraphPad Prism (GraphPad Software v.10) and are indicated in the figure legends. $P < 0.05$ is considered significant.

Ethics

Animal studies were performed according to approved protocols by the Institutional Animal Care and Use Committee (IACUC) of each institution in the US and the animal studies and protocols (permission numbers 16/2307 and 16/2372) were approved by the local government of Lower Saxony, Germany.

Extended Data

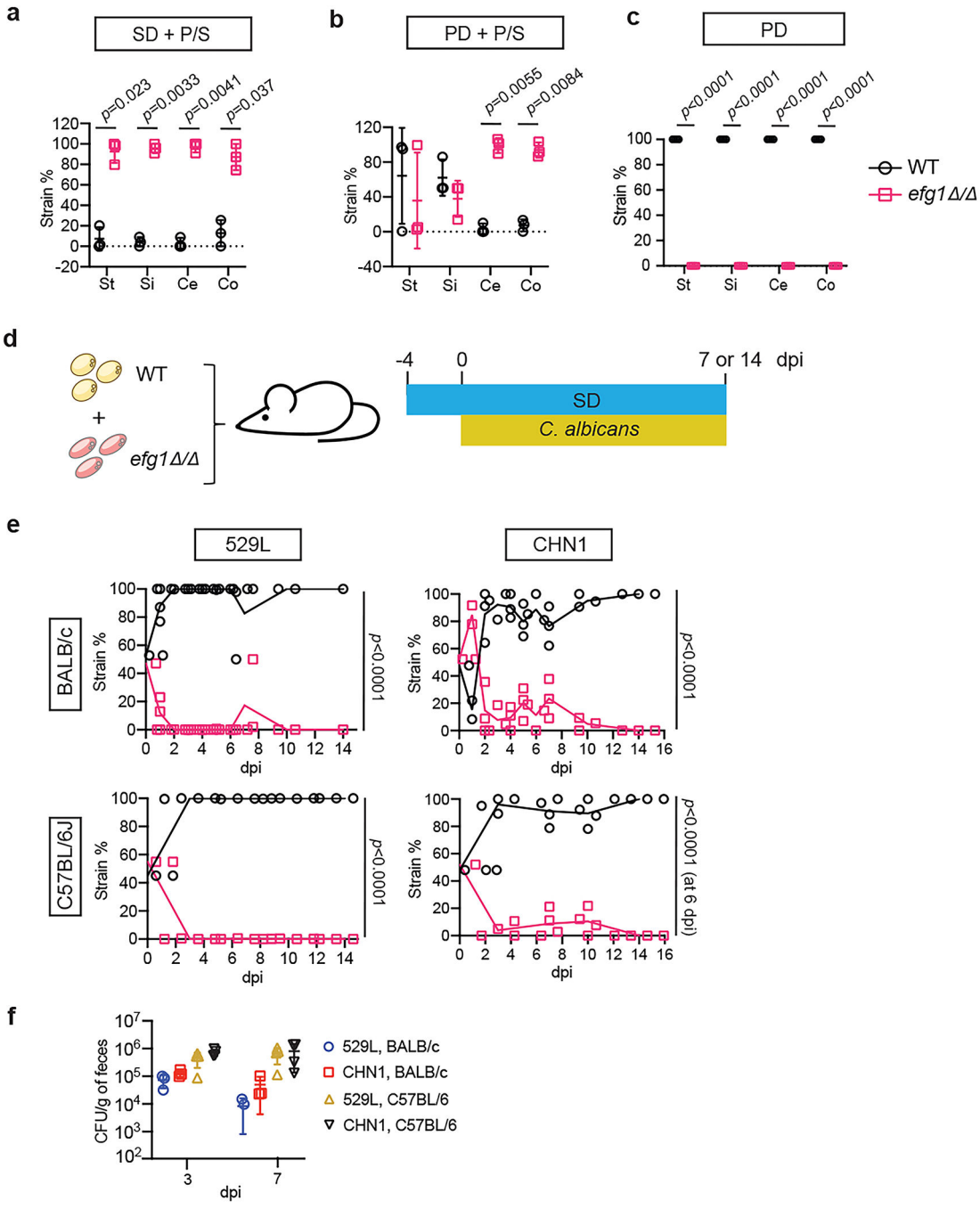

Extended Data Fig. 1|. Comparison of the fitness of WT and yeast-locked *efg1*Δ/Δ cells from different *C. albicans* strain backgrounds.

a, Experiments were performed as described in Fig.1. Mouse GI organs (St; stomach, Si; small intestine, Duo; duodenum, Je; jejunum, Ile; ileum, Ce; cecum, Co; colon) were homogenized to identify WT and *efg1Δ/Δ* cells 14 days post-*C. albicans* inoculation. WT (CAY2698) versus *efg1Δ/Δ* (CAY11750) competitions in SD+P/S (P/S; penicillin/streptomycin) model (**a**), PD+P/S model (**b**) and PD model (**c**). dpi; days post-inoculation.

d, Schematic of competition between WT and yeast-locked *efg1Δ/Δ* cells. Mice fed the SD without antibiotics were gavaged with a 1:1 mixture of WT and *efg1Δ/Δ* cells and *C. albicans* colonies were examined in fecal pellets at the indicated time points. **e**,**f**, Competition outcomes (**e**) and fecal CFUs (**f**) of WT versus *efg1Δ/Δ* in 529L (CAY5016 versus CAY11482) and CHN1 (CAY11170 versus CAY11184). Experiments were performed in BALB/c and C57BL/6J mice as indicated. Each data point represents an individual mouse, data are mean ± s.e.m in **a**, **b,** and **f**. $n = 3$ for competitions in BALB/c mice and $n = 4$ for competitions in C57BL/6J mice. A paired t-test (two-tailed) was used in **e** and a Mann-Whitney (two-tailed) test in **f**.

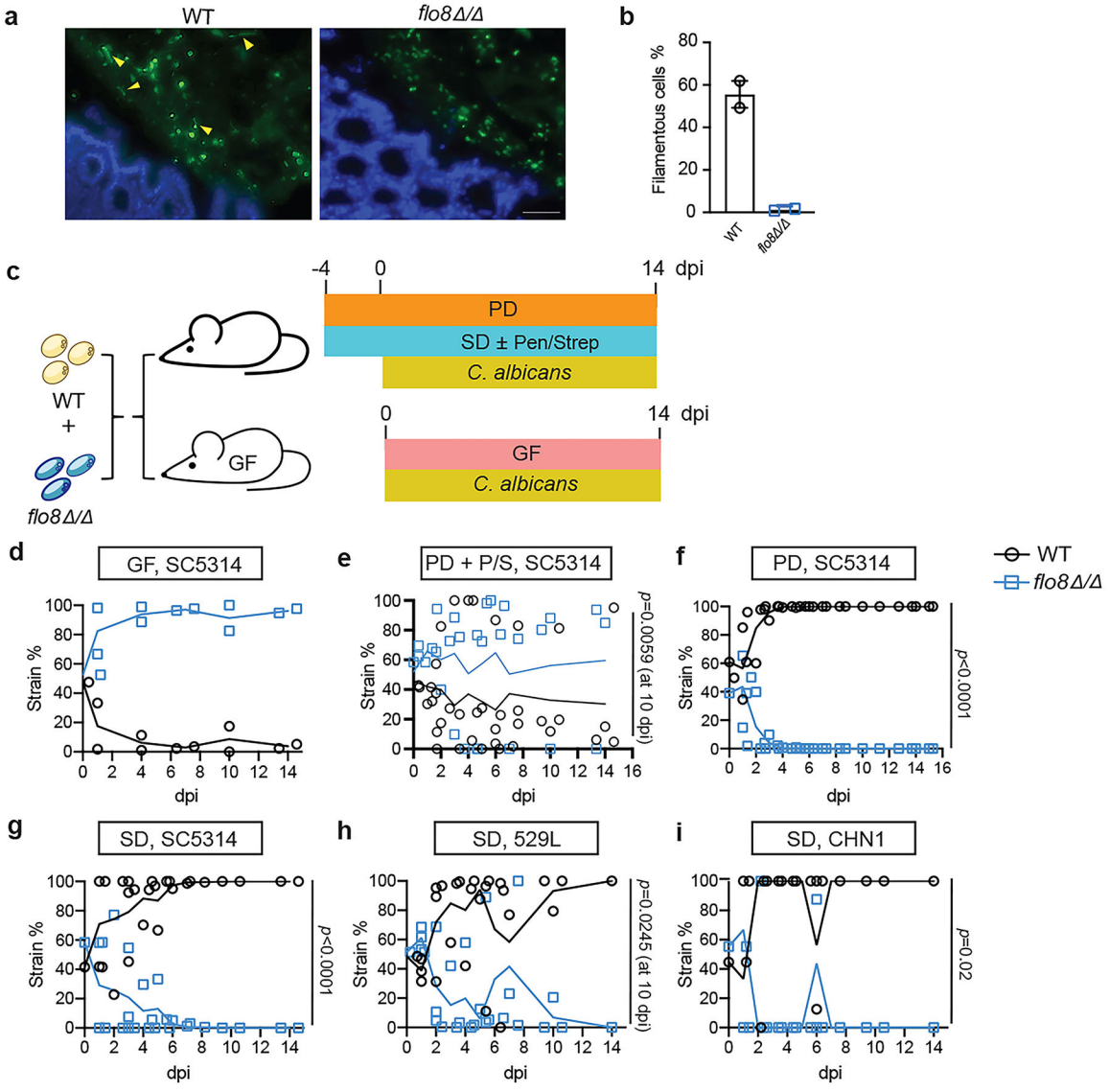

Extended Data Fig. 2|. Comparison of the fitness of WT and *flo8Δ/Δ* cells in different colonization models.

a, Microscopic images of cells in the colon of BALB/c SD+P/S mice infected with WT (CAY2698) or *flo8Δ/Δ* (CAY9796) cells at 7 days post-infection. **b**, Quantitative analysis

of yeast and filamentous morphotypes. *n* = 2. **c**, Schematic of competition between WT and *flo8Δ/Δ cells*. *n* = 2. Each data point represents an individual mouse. A 1:1 mix of WT and *flo8Δ/Δ* cells were inoculated by oral gavage and fecal samples were collected at the indicated time points. **d-f**, Results for SC5314 WT (CAY2698) versus *flo8Δ/Δ* (CAY9796) cells in GF BALB/c mice (**d**), conventional PD-fed BALB/c mice treated with antibiotics (P/S; penicillin/streptomycin) (**e**), and conventional PD-fed BALB/c mice (without antibiotics) (**f**). dpi; days post-inoculation. *n* = 3 in **e** and **f**. **g-i**, Competition of WT versus *flo8Δ/Δ* cells in BALB/c mice fed a SD (without antibiotics).. Experiments were performed using SC5314 (CAY2698 vs. CAY9796) (**g**), 529L (CAY11168 vs. CAY11180) (**h**), or CHN1 (CAY11170 vs. CAY11186) (**i**) strain backgrounds. *n* = 3. Each data point represents an individual mouse. Data are mean ± s.e.m in **b**. Significance was determined by a Mann-Whitney (two-tailed) test in **b** and a paired two-tailed t-test in **d-i**.

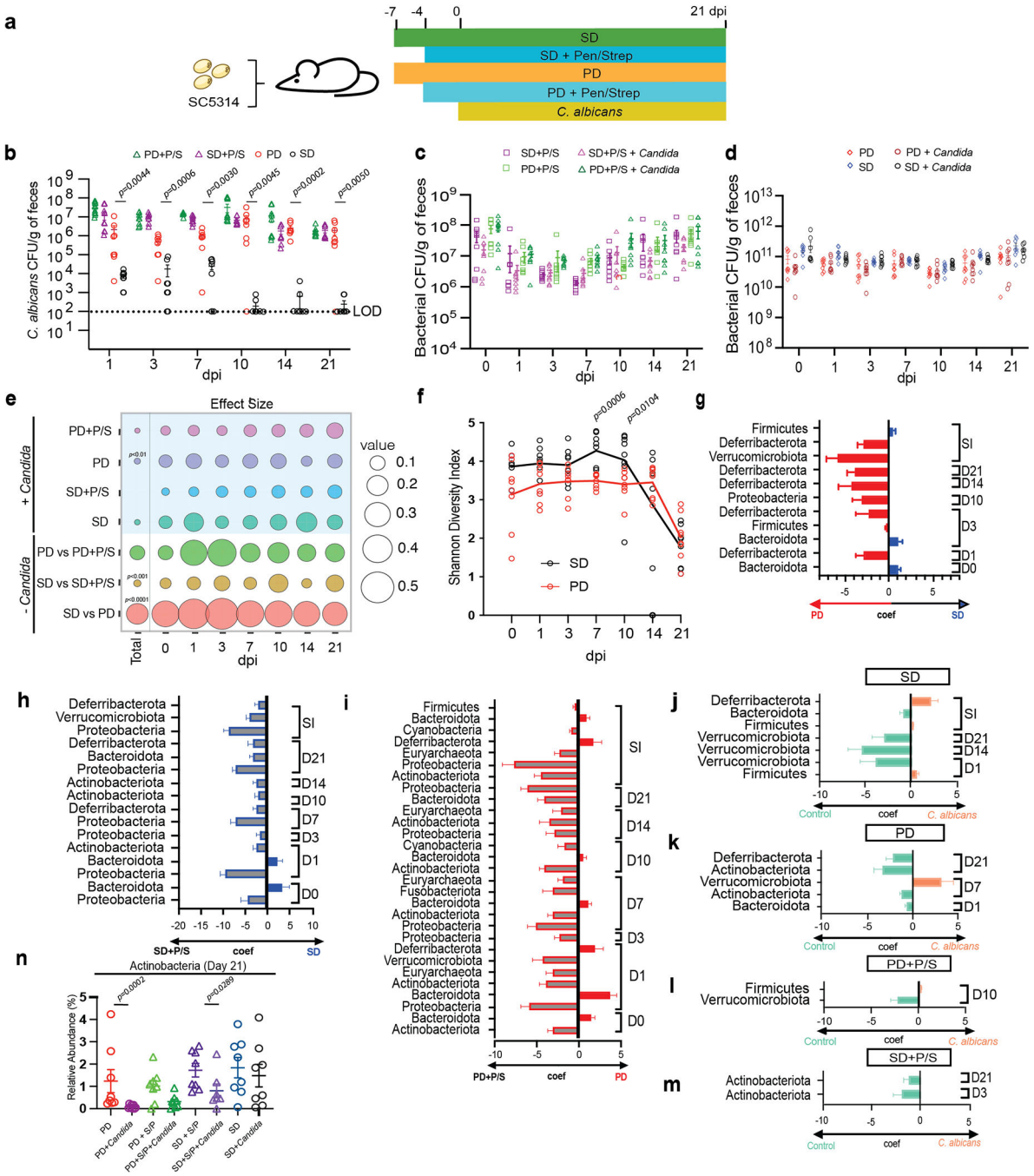

Extended Data Fig. 3|. Analysis of microbiome composition upon changes in diet, antibiotic treatment, and *C. albicans* colonization.

a, Schematic of colonization experiments. BALB/c mice were fed the SD or PD, with or without antibiotics (P/S; penicillin/streptomycin). These groups were compared with and without colonization with *C. albicans* SC5314 cells. **b**, *C. albicans* CFUs in fecal pellets collected at the indicated time points. LOD, limit of detection. $n = 8$. **c**,**d**, Total bacterial levels in fecal pellets collected at the indicated time points by quantitative PCR in SD- or PD-fed mice with antibiotics (**c**) and without antibiotics (**d**). $n = 8$. **e**, Bubble plot

depicting the amount of variation in gut microbial composition determined by Permutational Multivariate Analysis of Variance (PERMANOVA) analysis using the adonis function and Bray-Curtis distances of beta diversity. Effect size refers to the magnitude of the differences or dissimilarities between groups. **f**, Shannon diversity of control mice on SD or PD (n = 8). **g**-**m**, Distribution of bacterial phyla in different models as determined by MaAsLin2. PD vs. SD (**g**), SD vs. SD+P/S (**h**), PD vs. PD+P/S (**i**); (+/− *C. albicans*) SD (**j**), PD (**k**), PD+P/S (**l**) and SD+P/S (**m**). Coefficient with standard error shown on x-axis. adj p-val cutoff 0.05. **n**, Relative abundance of Actinobacteria across different diet fed mice (+/− *Candida*) groups on Day 21. n = 8. Each data point represents an individual mouse. Data are mean ± s.e.m in **b**-**m**. A Mann-Whitney test was used in **b**,**f**,and **n**.

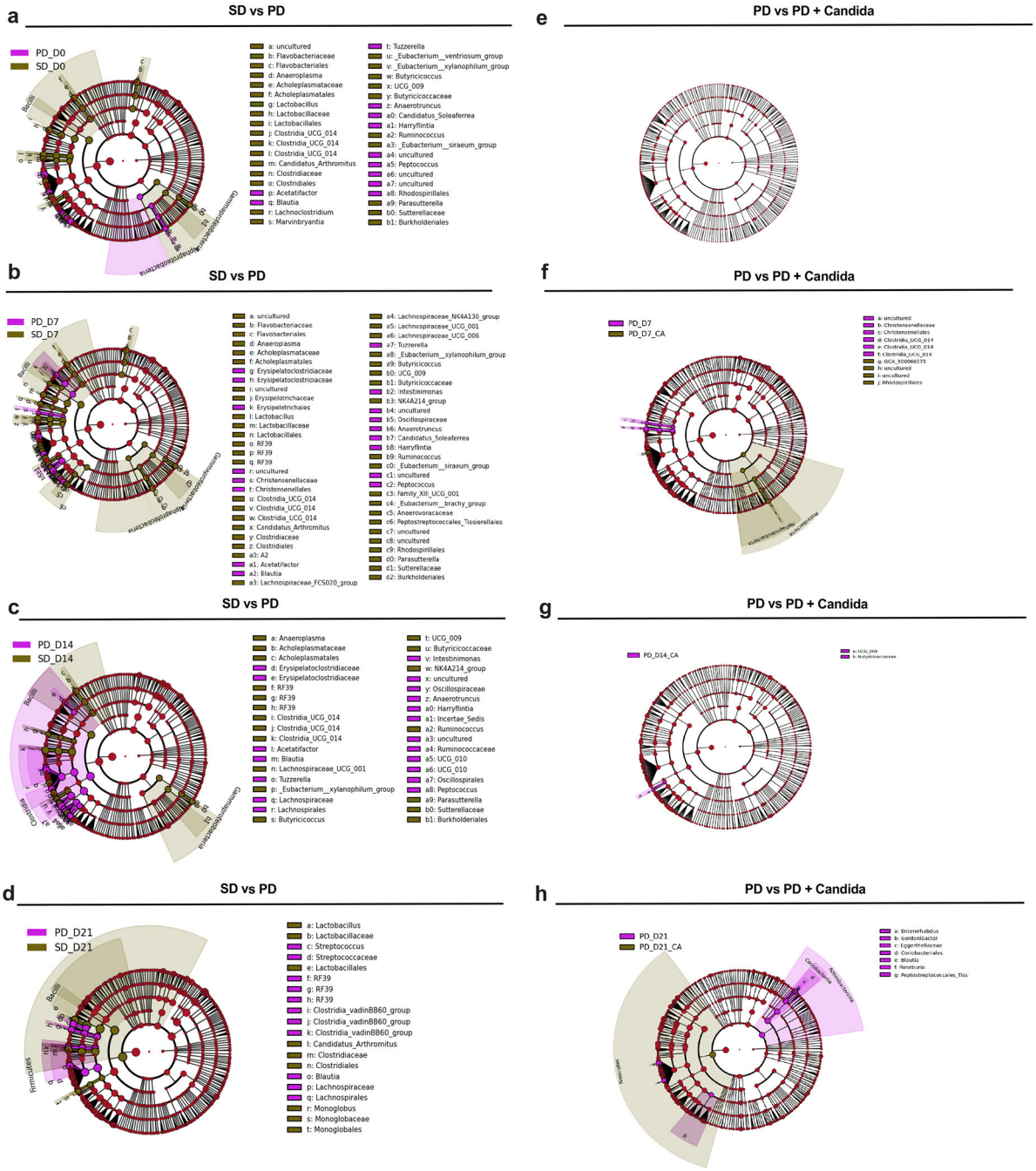

Extended Data Fig. 4|. Linear discriminant analysis Effect Size (LEfSe) analysis to compare the alterations in gut bacterial populations in mice on different diets.

Linear discriminant analysis (LDA) effect size for significant taxa in the microbiome of mice fed the SD vs. PD are plotted onto a cladogram for Day 0 (**a**), Day 7 (**b**), Day 14 (**c**), Day 21 (**d**). and for mice fed the PD (+/− *C. albicans*) for Day 0 (**e**), Day 7 (**f**), Day 14 (**g**) and Day 21 (**h**). Analysis was performed on mice as shown in Extended Data Fig. 3 (n=8 per group). Differentially abundant species with LDA score >2 are shown in nodes represented with red (PD) and green (SD) and non-significant species are represented with yellow. A

Kruskal-Wallis test was used to compare features between diets (p<0.05) and the Pairwise Wilcoxon test was used to compare between taxa (p<0.05).

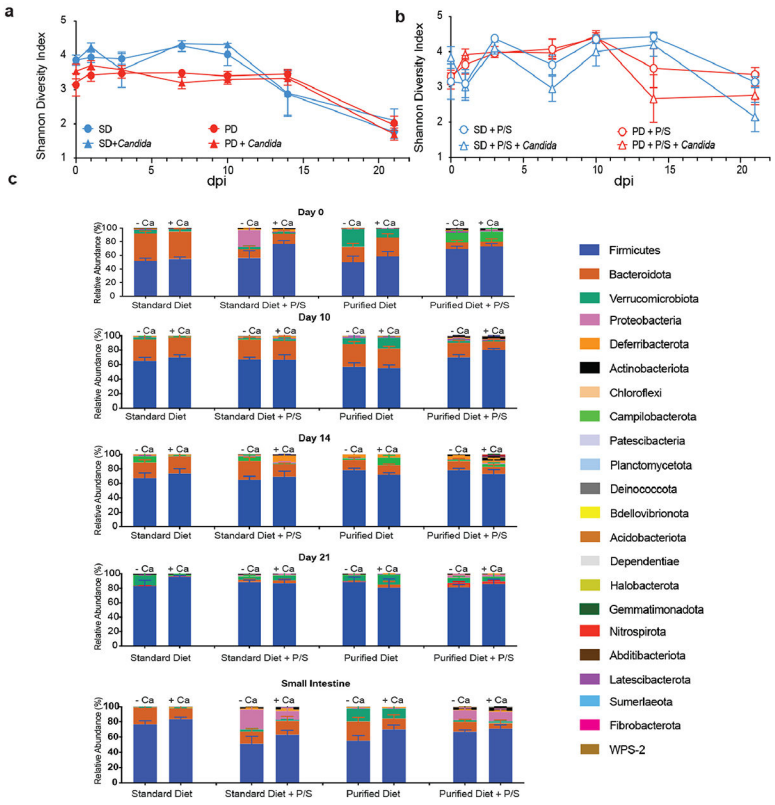

Extended Data Fig. 5|. Analysis of gut bacterial populations in different murine models. 16S rRNA sequencing data was used to determine the relative abundance of bacterial phyla in BALB/c colonization experiments using mice fed the SD or PD, and supplemented or not supplemented with antibiotics (P/S; penicillin/streptomycin). Each group of mice were also compared +/− inoculation with *C. albicans* SC5314 cells, as shown in Extended Data Fig. 3. **a**,**b**, Shannon diversity for bacterial populations from fecal pellets for the shown experiments. n = 8. **c**, Relative abundance of bacteria shown for fecal pellets on days 0, 10, 14, and 21, and for the small intestine at day 21. n = 8. Data are mean ± s.e.m in **a**-**c**.

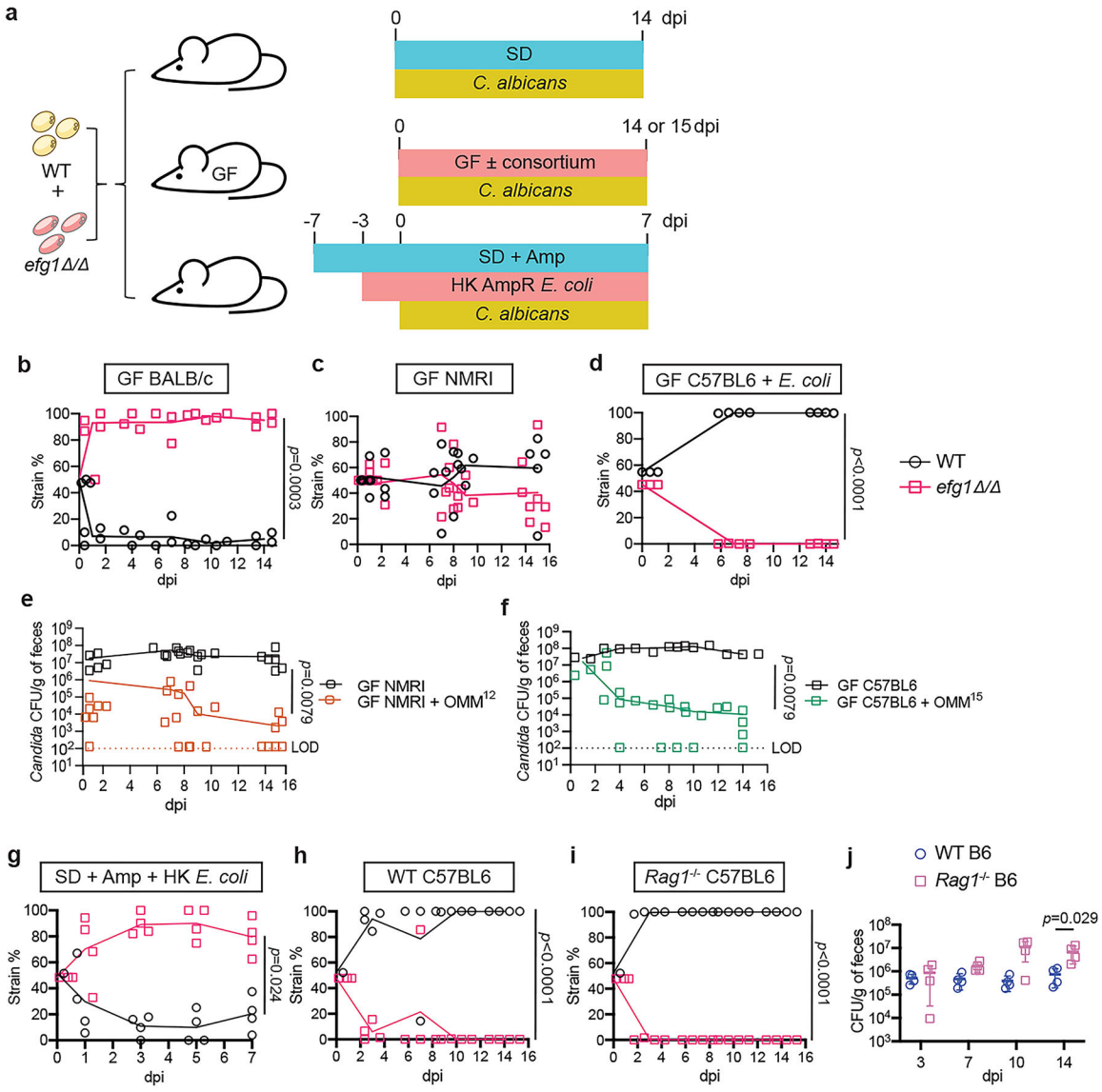

Extended Data Fig. 6|. *C. albicans* WT cells outcompete *efg1Δ/Δ* cells in gnotobiotic mice harboring different bacterial populations.

a, Schematic of competition between WT and yeast-locked *efg1Δ/Δ* cells in gnotobiotic colonization models. Mice were gavaged with a 1:1 mixture of WT SC5314 (CAY2698) and *efg1Δ/Δ* (CAY11750) cells. **b-d**, *C. albicans* cells were tested in GF BALB/c mice (**b**), GF NMRI mice (**c**), or GF C57BL/6 mice colonized with *E. coli* prior to inoculation with *C. albicans* (**d**). $n = 4$ in **b**, 8 in **c**, and 5 in **d**. **e**, *C. albicans* CFUs in fecal pellets collected at the indicated time points in GF NMRI mice (**e**) and GF C57BL/6 mice (**f**). $n = 8$ in **e**, $n = 3–5$ in **f**. LOD, limit of detection. **g**, WT v. *efg1Δ/Δ* competition in Amp-treated mice gavaged with heat-killed AmpR *E. coli*. $n = 4$. **h**,**i**, Competition between CHN1 WT (CAY11170) and *efg1*Δ/Δ (CAY11184) cells in WT mice (**h**) or *Rag1*$^{-/-}$ mice (**i**) on the SD (no antibiotics). $n = 4$. **j**, *C. albicans* CFU levels in the fecal pellets from WT and *Rag1*$^{-/-}$ mice. $n = 4$. Each data point represents an individual mouse. Data are mean ± s.e.m in **j**. A

paired t-test (two-tailed) was used in **b**-**d** and **g**-**i**, and a Mann-Whitney (two-tailed) test in **e**,**f** and **j**.

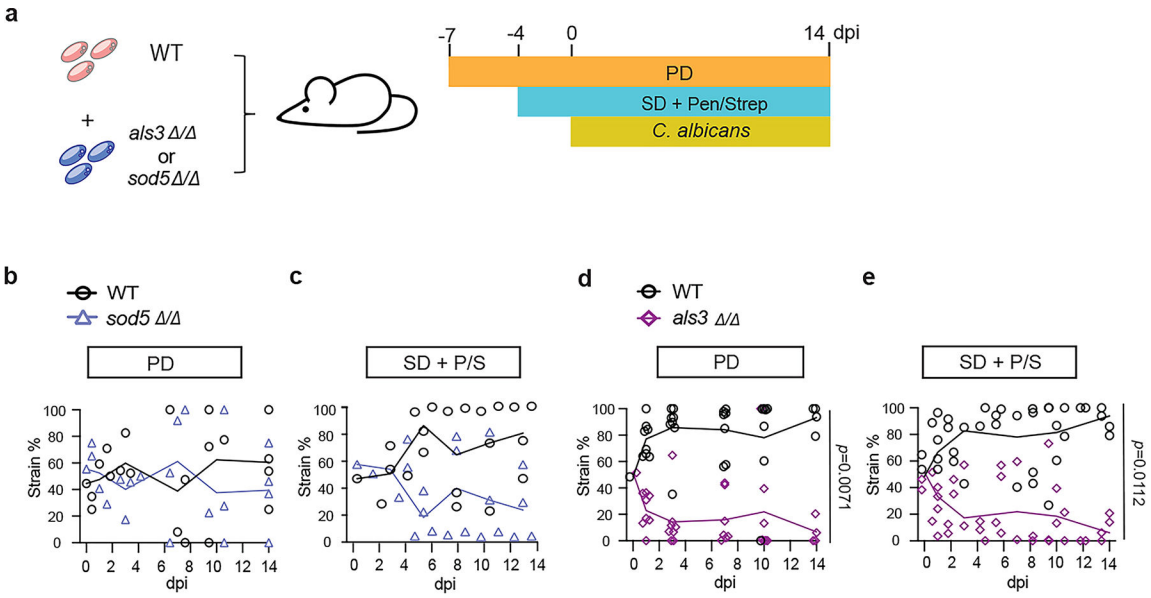

Extended Data Fig.7|. Examining the role of *ALS3* and *SOD5* in GI colonization fitness.

a, Schematic of competition between WT *C. albicans* and *sod5Δ/Δ* or *als3Δ/Δ* cells (SC5314 background). **b**-**e**, BALB/c mice fed a PD without antibiotics or a SD with antibiotics (P/S; penicillin/streptomycin). Experiments used WT (CAY8785) and *sod5Δ/Δ* (CAY14738) in **b** and **c**. $n = 4$. WT (CAY8785) and *als3Δ/Δ* (CAY14696) in **d** and **e**. $n = 8$. Each data point represents an individual mouse. A paired t-test (two-tailed) was used for statistical significance.

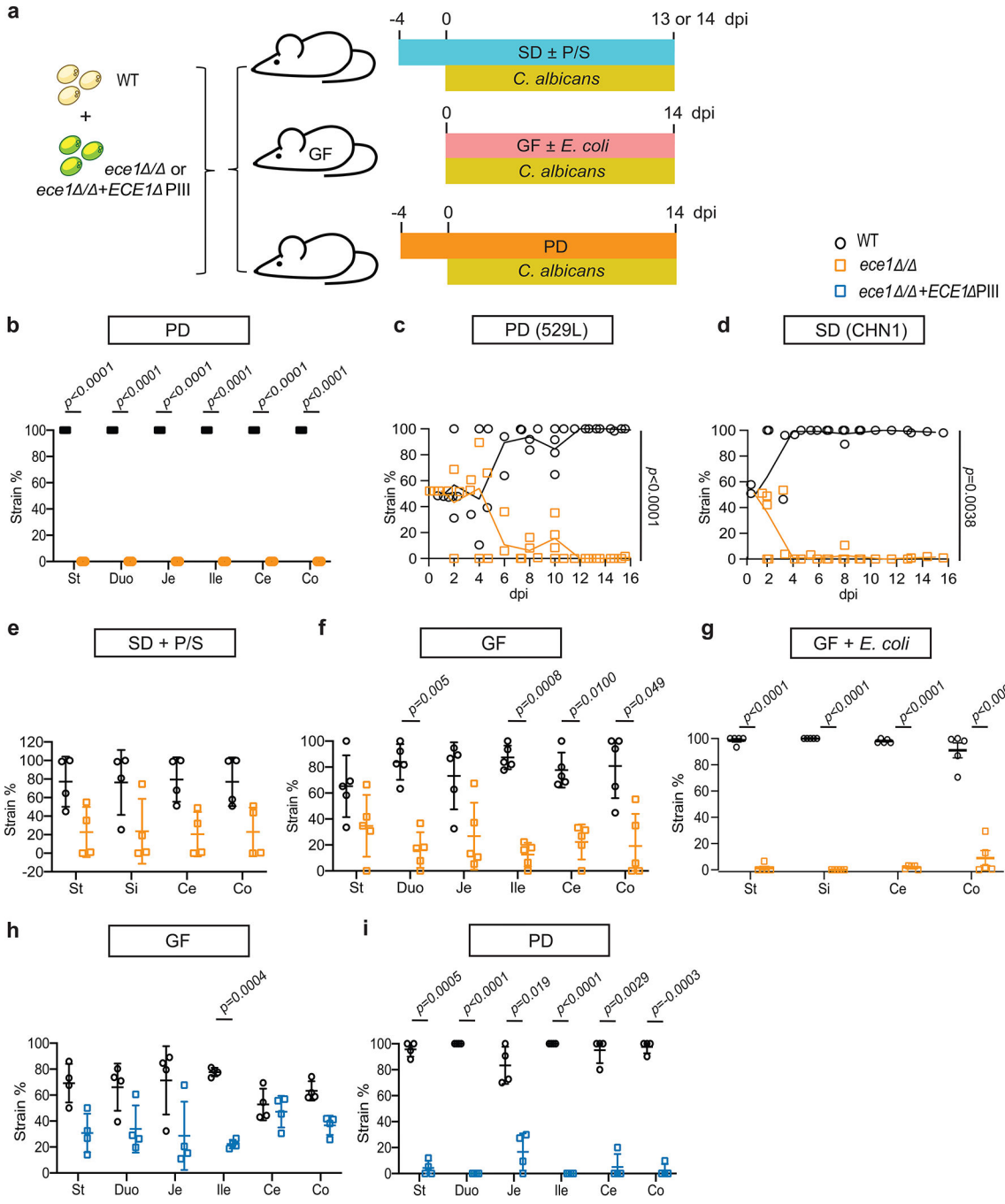

Extended Data Fig. 8|. Colonization fitness of WT and *ece1Δ/Δ* mutants.

Experiments were performed as described in Fig. 4. Mouse GI organs (St; stomach, Si; small intestine, Duo; duodenum, Je; jejunum, Ile; ileum, Ce; cecum, Co; colon) were homogenized to identify the ratio of WT and *ece1Δ/Δ* cells 14 days post *C. albicans* infection. **b**, Competition between CAY11533 (WT) versus CAY11507 (*ece1Δ/Δ*) cells in BALB/c fed a PD. $n = 5$. **c**, Competition between WT (CAY11168) and *ece1Δ/Δ* cells (CAY12441) in the 529L background BALB/c mice fed a PD. $n = 4$. **d**, Competition between WT (CAY11170) and *ece1Δ/Δ cells* (CAY12446) in the CHN1 background in SD-fed BALB/c mice. $n =$

4. **e-g**, Competition between CAY12202 (WT) versus CAY8578 (*ece1Δ/Δ*) BALB/c mice fed a SD plus antibiotics (P/S; penicillin/streptomycin) (**e**), GF C57BL/6 mice (**f**), and GF C57BL/6 mice colonized with *E. coli* prior to *C. albicans* inoculation (**g**). $n = 4$ in **e**, and 5 in **f** and **g.** Competition outcomes of WT (CAY12202) versus e*ce1Δ/Δ+ECE1ΔpIII* (CAY8580) in GF C57BL/6 mice (**h**) and in BALB/c mice fed a PD (**i**). $n = 4$ in **h** and **i**. Each data point represents an individual mouse. Data are mean ± s.e.m in **c** – **e, h, i**. A paired t-test (two-tailed) was used to determine the significance between two populations (**b**-**h**).

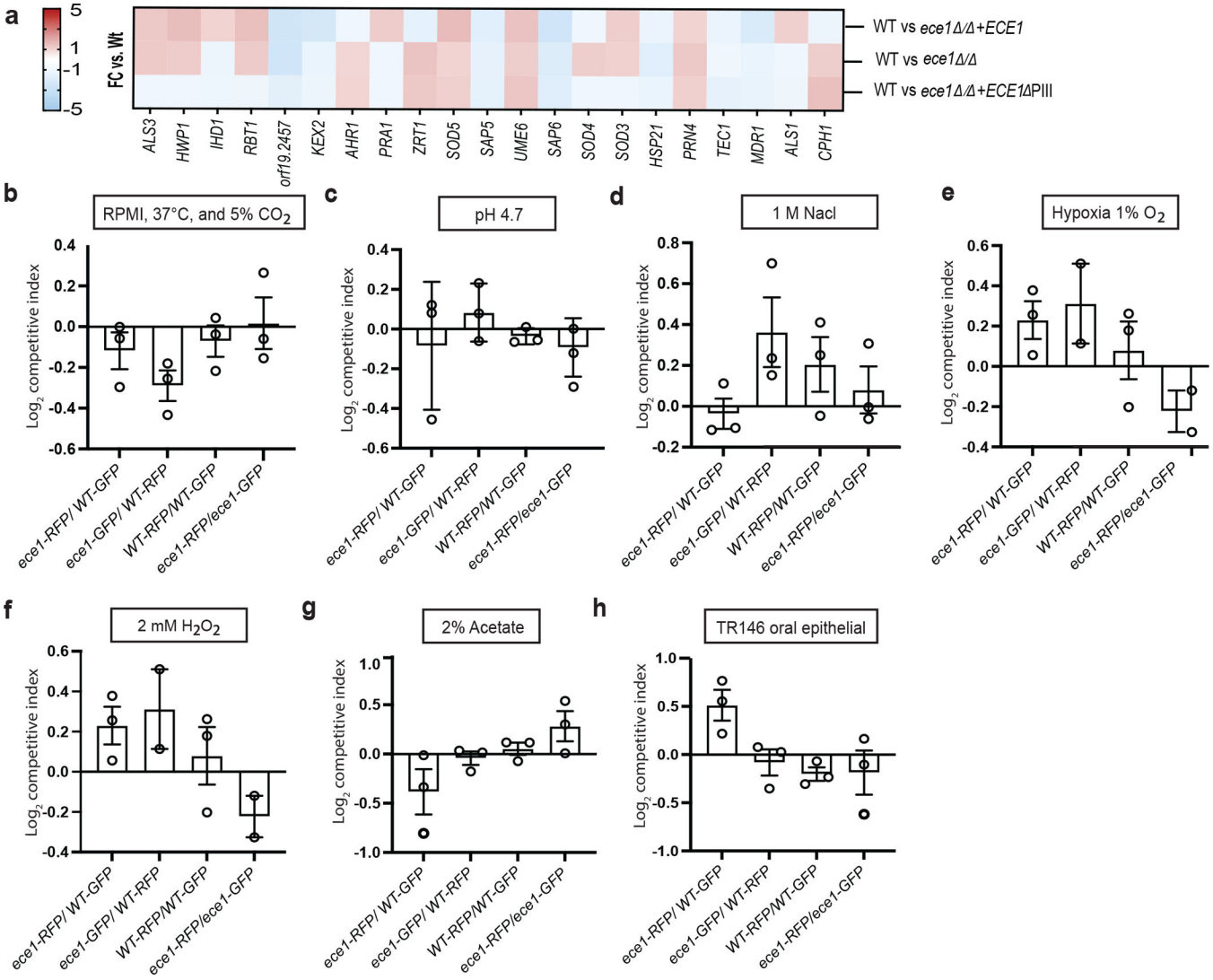

Extended Data Fig. 9|. Comparison of *C. albicans* WT and *ece1Δ/Δ* cells *in vitro*.
a, Heat map of transcriptome analysis representing the fold change (FC) in expression of fungal genes when strains were grown under hyphal-inducing conditions (3 h, 37°C, 5% CO_2). **b-h**, Competitive fitness of SC5314 WT and *ece1Δ/Δ* cells in RPMI (37°C, 5% CO_2) (**b**), acidic pH (pH 4.7) (**c**), high salt (1 M NaCl) (**d**), hypoxia (1% O_2) (**e**), oxidative stress (2 mM H_2O_2) (**f**), in the presence of 1% acetate (**g**), and during incubation with TR146 epithelial cells (**h**). Competitive index was calculated using the formula: $\log_2$

[($MUT_{competition}$/$WT_{competition}$)/ (MUT_{single}/WT_{single})]. Fitness of the *ece1Δ/Δ* relative to the WT is represented as $\log_2$ competitive index. Data are representative of three biological replicates (n = 3). Graphs show the mean ± SEM in **b** - **h**. Statistical analysis was performed using 1-way ANOVA with Bonferroni post hoc test to detect significance.

Supplementary Material

Refer to Web version on PubMed Central for supplementary material.

Acknowledgements

This work was supported by NIH grants AI166869, AI141893, AI081704 and AI168222 to R.J.B. Y-H.C. was supported by the Charles H. Revson Senior Fellowship in Biomedical Science. B.H. and T.B.S. were supported by the German Research Foundation (Deutsche Forschungsgemeinschaft, DFG) within the Cluster of Excellence "Balance of the Microverse", under Germany's Excellence Strategy – EXC 2051 –Project-ID 390713860. B.H. and S.A. were further supported by the DFG, project HU 528/20-1. J.C.P was supported by AI175081, P.B. was supported by DK125382 and S.P. was supported by a Graduate Research Fellowship from the NSF under award number 1644760. I.V.E. was supported by the Institut Pasteur and is a CIFAR Azrieli Global Scholar in the CIFAR Program Fungal Kingdom: Threats & Opportunities. We thank Eric Pamer, Ilse Jacobsen and Tobias Hohl for sharing strains and the support of the National Gnotobiotic Rodent Resource Center.

Data Availability

16S sequencing data are publicly available at the NCBI Sequence Read Archive (SRA) and can be accessed under BioProject PRJNA1008281. Microarray data for analysis of *C. albicans* expression are available at ArrayExpress under accession MTAB-13349. Source data that reproduce the plots in the main figures (Fig. 1–4) and Extended Data figures (Fig. 1–9) are provided with this paper.

References

1. Ost KS et al. Adaptive immunity induces mutualism between commensal eukaryotes. Nature 596, 114–118, doi:10.1038/s41586-021-03722-w (2021). [PubMed: 34262174]
2. Tso GHW et al. Experimental evolution of a fungal pathogen into a gut symbiont. Science 362, 589–595, doi:10.1126/science.aat0537 (2018). [PubMed: 30385579]
3. Witchley JN et al. *Candida albicans* morphogenesis programs control the balance between gut commensalism and invasive infection. Cell Host Microbe 25, 432–443 e436, doi:10.1016/j.chom.2019.02.008 (2019). [PubMed: 30870623]
4. Moyes DL et al. Candidalysin is a fungal peptide toxin critical for mucosal infection. Nature 532, 64–68, doi:10.1038/nature17625 (2016). [PubMed: 27027296]
5. Li XV et al. Immune regulation by fungal strain diversity in inflammatory bowel disease. Nature, doi:10.1038/s41586-022-04502-w (2022).
6. Doron I et al. Mycobiota-induced IgA antibodies regulate fungal commensalism in the gut and are dysregulated in Crohn's disease. Nat Microbiol 6, 1493–1504, doi:10.1038/s41564-021-00983-z (2021). [PubMed: 34811531]
7. Rao C et al. Multi-kingdom ecological drivers of microbiota assembly in preterm infants. Nature 591, 633–638, doi:10.1038/s41586-021-03241-8 (2021). [PubMed: 33627867]
8. Iliev ID & Cadwell K Effects of intestinal fungi and viruses on immune responses and inflammatory bowel diseases. Gastroenterology 160, 1050–1066, doi:10.1053/j.gastro.2020.06.100 (2021). [PubMed: 33347881]
9. Swidergall M & LeibundGut-Landmann S Immunosurveillance of Candida albicans commensalism by the adaptive immune system. Mucosal Immunol 15, 829–836, doi:10.1038/s41385-022-00536-5 (2022). [PubMed: 35778599]

10. Shao TY, Haslam DB, Bennett RJ & Way SS Friendly fungi: symbiosis with commensal *Candida albicans*. Trends in Immunology 43, 706–717, doi:10.1016/j.it.2022.07.003 (2022). [PubMed: 35961916]
11. Li Q et al. Dysbiosis of gut fungal microbiota is associated with mucosal inflammation in Crohn's disease. J Clin Gastroenterol 48, 513–523, doi:10.1097/MCG.0000000000000035 (2014). [PubMed: 24275714]
12. Sokol H et al. Fungal microbiota dysbiosis in IBD. Gut 66, 1039–1048, doi:10.1136/gutjnl-2015-310746 (2017). [PubMed: 26843508]
13. Bacher P et al. Human Anti-fungal Th17 immunity and pathology rely on cross-reactivity against *Candida albicans*. Cell 176, 1340–1355 e1315, doi:10.1016/j.cell.2019.01.041 (2019). [PubMed: 30799037]
14. Shao TY et al. Commensal *Candida albicans* positively calibrates systemic Th17 immunological responses. Cell Host Microbe 25, 404–417 e406, doi:10.1016/j.chom.2019.02.004 (2019). [PubMed: 30870622]
15. Yeung F et al. Altered immunity of laboratory mice in the natural environment is associated with fungal colonization. Cell Host Microbe 27, 809–822 e806, doi:10.1016/j.chom.2020.02.015 (2020). [PubMed: 32209432]
16. Zhai B et al. High-resolution mycobiota analysis reveals dynamic intestinal translocation preceding invasive candidiasis. Nature Medicine 26, 59–64, doi:10.1038/s41591-019-0709-7 (2020).
17. Pappas PG, Lionakis MS, Arendrup MC, Ostrosky-Zeichner L & Kullberg BJ Invasive candidiasis. Nat Rev Dis Primers 4, 18026, doi:10.1038/nrdp.2018.26 (2018). [PubMed: 29749387]
18. Koh AY, Kohler JR, Coggshall KT, Van Rooijen N & Pier GB Mucosal damage and neutropenia are required for Candida albicans dissemination. PLoS Pathog 4, e35 (2008). [PubMed: 18282097]
19. Noble SM, Gianetti BA & Witchley JN *Candida albicans* cell-type switching and functional plasticity in the mammalian host. Nat Rev Microbiol 15, 96–108, doi:10.1038/nrmicro.2016.157 (2017). [PubMed: 27867199]
20. Kadosh D in Candida albicans: Cellular and Molecular Biology (ed Rajendra Prasad) 41–62 (Springer International Publishing, 2017).
21. Saville SP, Lazzell AL, Monteagudo C & Lopez-Ribot JL Engineered control of cell morphology *in vivo* reveals distinct roles for yeast and filamentous forms of *Candida albicans* during infection. Eukaryot Cell 2, 1053–1060 (2003). [PubMed: 14555488]
22. Lo HJ et al. Nonfilamentous *C. albicans* mutants are avirulent. Cell 90, 939–949, doi:S0092-8674(00)80358-X [pii] (1997). [PubMed: 9298905]
23. Carlisle PL et al. Expression levels of a filament-specific transcriptional regulator are sufficient to determine *Candida albicans* morphology and virulence. Proc Natl Acad Sci U S A 106, 599–604, doi:0804061106 [pii]10.1073/pnas.0804061106 (2009). [PubMed: 19116272]
24. Bohm L et al. The yeast form of the fungus *Candida albicans* promotes persistence in the gut of gnotobiotic mice. PLoS Pathog 13, e1006699, doi:10.1371/journal.ppat.1006699 (2017). [PubMed: 29069103]
25. Liang SH et al. Hemizygosity enables a mutational transition governing fungal virulence and commensalism. Cell Host Microbe 25, 418–431 e416, doi:10.1016/j.chom.2019.01.005 (2019). [PubMed: 30824263]
26. Mogavero S et al. Candidalysin delivery to the invasion pocket is critical for host epithelial damage induced by *Candida albicans*. Cell Microbiol 23, e13378, doi:10.1111/cmi.13378 (2021). [PubMed: 34245079]
27. Naglik JR, Gaffen SL & Hube B Candidalysin: discovery and function in *Candida albicans* infections. Curr Opin Microbiol 52, 100–109, doi:10.1016/j.mib.2019.06.002 (2019). [PubMed: 31288097]
28. Stoldt VR, Sonneborn A, Leuker CE & Ernst JF Efg1p, an essential regulator of morphogenesis of the human pathogen *Candida albicans*, is a member of a conserved class of bHLH proteins regulating morphogenetic processes in fungi. EMBO J 16, 1982–1991, doi:10.1093/emboj/16.8.1982 (1997). [PubMed: 9155024]
29. Braun BR & Johnson AD *TUP1, CPH1* and *EFG1* make independent contributions to filamentation in *Candida albicans*. Genetics 155, 57–67. (2000). [PubMed: 10790384]

30. Wakade RS, Huang M, Mitchell AP, Wellington M & Krysan DJ Intravital imaging of *Candida albicans* identifies differential *in vitro* and *in vivo* filamentation phenotypes for transcription factor deletion mutants. mSphere 6, e0043621, doi:10.1128/mSphere.00436-21 (2021). [PubMed: 34160243]
31. Fan D et al. Activation of HIF-1alpha and LL-37 by commensal bacteria inhibits C*andida albicans* colonization. Nature Medicine 21, 808–814, doi:10.1038/nm.3871 (2015).
32. Yamaguchi N et al. Gastric colonization of *Candida albicans* differs in mice fed commercial and purified diets. J Nutr 135, 109–115, doi:135/1/109 [pii] (2005). [PubMed: 15623841]
33. Liang SH et al. Hemizygosity enables a mutational transition governing fungal virulence and commensalism. Cell Host Microbe 25, 418–431.e416, doi:10.1016/j.chom.2019.01.005 (2019). [PubMed: 30824263]
34. McDonough LD et al. Candida albicans isolates 529L and CHN1 exhibit stable colonization of the murine gastrointestinal tract. mBio 12, e0287821, doi:10.1128/mBio.02878-21 (2021). [PubMed: 34724818]
35. Braun BR, Kadosh D & Johnson AD *NRG1*, a repressor of filamentous growth in *C. albicans*, is down-regulated during filament induction. Embo J 20, 4753–4761. (2001). [PubMed: 11532939]
36. Murad AM et al. *NRG1* represses yeast-hypha morphogenesis and hypha-specific gene expression in *Candida albicans*. Embo J 20, 4742–4752. (2001). [PubMed: 11532938]
37. Wakade RS, Kramara J, Wellington M & Krysan DJ *Candida albicans* filamentation does not require the cAMP-PKA pathway *in vivo*. mBio, e0085122, doi:10.1128/mbio.00851-22 (2022). [PubMed: 35475642]
38. Vautier S et al. *Candida albicans* colonization and dissemination from the murine gastrointestinal tract: the influence of morphology and Th17 immunity. Cell Microbiol 17, 445–450, doi:10.1111/cmi.12388 (2015). [PubMed: 25346172]
39. Miller BM, Liou MJ, Lee JY & Baumler AJ The longitudinal and cross-sectional heterogeneity of the intestinal microbiota. Curr Opin Microbiol 63, 221–230, doi:10.1016/j.mib.2021.08.004 (2021). [PubMed: 34428628]
40. Brugiroux S et al. Genome-guided design of a defined mouse microbiota that confers colonization resistance against Salmonella enterica serovar Typhimurium. Nat Microbiol 2, 16215, doi:10.1038/nmicrobiol.2016.215 (2016). [PubMed: 27869789]
41. Trexler PC, Hon D & Orcutt R in Development of Gnotobiotics and contamination control in laboratory animal science introduction: nomenclature (American Association for Laboratory Animal Science Memphis, TN, 1999).
42. Caballero S et al. Cooperating commensals restore colonization resistance to vancomycin-resistant *Enterococcus faecium*. Cell Host Microbe 21, 592–602 e594, doi:10.1016/j.chom.2017.04.002 (2017). [PubMed: 28494240]
43. Dambuza IM & Brown GD Managing the mycobiota with IgA. Nat Microbiol 6, 1471–1472, doi:10.1038/s41564-021-01006-7 (2021). [PubMed: 34811532]
44. Kasper L et al. The fungal peptide toxin Candidalysin activates the NLRP3 inflammasome and causes cytolysis in mononuclear phagocytes. Nature Communications 9, 4260, doi:10.1038/s41467-018-06607-1 (2018).
45. Swidergall M et al. Candidalysin is required for neutrophil recruitment and virulence during systemic *Candida albicans* infection. J Infect Dis 220, 1477–1488, doi:10.1093/infdis/jiz322 (2019). [PubMed: 31401652]
46. White SJ et al. Self-regulation of Candida albicans population size during GI colonization. PLoS Pathog 3, e184, doi:10.1371/journal.ppat.0030184 (2007). [PubMed: 18069889]
47. Hoyer LL, Payne TL, Bell M, Myers AM & Scherer S *Candida albicans ALS3* and insights into the nature of the *ALS* gene family. Curr Genet 33, 451–459, doi:10.1007/s002940050359 (1998). [PubMed: 9644209]
48. Phan QT et al. Als3 is a *Candida albicans* invasin that binds to cadherins and induces endocytosis by host cells. PLoS Biol 5, e64 (2007). [PubMed: 17311474]
49. Almeida RS et al. the hyphal-associated adhesin and invasin Als3 of *Candida albicans* mediates iron acquisition from host ferritin. PLoS Pathog 4, e1000217, doi:10.1371/journal.ppat.1000217 (2008). [PubMed: 19023418]

50. Martchenko M, Alarco AM, Harcus D & Whiteway M Superoxide dismutases in *Candida albicans*: transcriptional regulation and functional characterization of the hyphal-induced *SOD5* gene. Mol Biol Cell 15, 456–467, doi:10.1091/mbc.e03-03-0179 (2004). [PubMed: 14617819]

51. Fradin C et al. Granulocytes govern the transcriptional response, morphology and proliferation of *Candida albicans* in human blood. Mol Microbiol 56, 397–415, doi:10.1111/j.1365-2958.2005.04557.x (2005). [PubMed: 15813733]

52. Hube B Fungal adaptation to the host environment. Curr Opin Microbiol 12, 347–349, doi:10.1016/j.mib.2009.06.009 (2009). [PubMed: 19577508]

Additional references

53. Dewhirst FE et al. Phylogeny of the defined murine microbiota: altered Schaedler flora. Appl Environ Microbiol 65, 3287–3292, doi:10.1128/AEM.65.8.3287-3292.1999 (1999). [PubMed: 10427008]

54. Guthrie C & Fink GR Guide to Yeast Genetics and Molecular Biology. (Academic Press, 1991).

55. Liu H, Kohler J & Fink GR Suppression of hyphal formation in *Candida albicans* by mutation of a *STE12* homolog. Science 266, 1723–1726 (1994). [PubMed: 7992058]

56. Park SO, Frazer C & Bennett RJ An adjuvant-based approach enables the use of dominant HYG and KAN selectable markers in Candida albicans. mSphere 7, e0034722, doi:10.1128/msphere.00347-22 (2022). [PubMed: 35968963]

57. Reuss O, Vik A, Kolter R & Morschhauser J The *SAT1* flipper, an optimized tool for gene disruption in *Candida albicans*. Gene 341, 119–127 (2004). [PubMed: 15474295]

58. Noble SM & Johnson AD Strains and strategies for large-scale gene deletion studies of the diploid human fungal pathogen *Candida albicans*. Eukaryot Cell 4, 298–309 (2005). [PubMed: 15701792]

59. Mancera E et al. Genetic modification of closely related *Candida* species. Frontiers in Microbiology 10, 357, doi:10.3389/fmicb.2019.00357 (2019). [PubMed: 30941104]

60. Gerami-Nejad M, Zacchi LF, McClellan M, Matter K & Berman J Shuttle vectors for facile gap repair cloning and integration into a neutral locus in *Candida albicans*. Microbiology 159, 565–579, doi:10.1099/mic.0.064097-0 (2013). [PubMed: 23306673]

61. Hollomon JM et al. The Candida albicans Cdk8-dependent phosphoproteome reveals repression of hyphal growth through a Flo8-dependent pathway. PLoS Genet 18, e1009622, doi:10.1371/journal.pgen.1009622 (2022). [PubMed: 34982775]

62. Dallari S et al. Enteric viruses evoke broad host immune responses resembling those elicited by the bacterial microbiome. Cell Host Microbe 29, 1014–1029 e1018, doi:10.1016/j.chom.2021.03.015 (2021). [PubMed: 33894129]

63. Thompson LR et al. A communal catalogue reveals Earth's multiscale microbial diversity. Nature 551, 457–463, doi:10.1038/nature24621 (2017). [PubMed: 29088705]

64. Callahan BJ et al. DADA2: High-resolution sample inference from Illumina amplicon data. Nature Methods 13, 581–583, doi:10.1038/nmeth.3869 (2016). [PubMed: 27214047]

65. Bolyen E et al. Reproducible, interactive, scalable and extensible microbiome data science using QIIME 2. Nat Biotechnol 37, 852–857, doi:10.1038/s41587-019-0209-9 (2019). [PubMed: 31341288]

66. Katoh K, Misawa K, Kuma K & Miyata T MAFFT: a novel method for rapid multiple sequence alignment based on fast Fourier transform. Nucleic Acids Res 30, 3059–3066, doi:10.1093/nar/gkf436 (2002). [PubMed: 12136088]

67. Price MN, Dehal PS & Arkin AP FastTree 2--approximately maximum-likelihood trees for large alignments. PLoS One 5, e9490, doi:10.1371/journal.pone.0009490 (2010). [PubMed: 20224823]

68. Bokulich NA et al. q2-longitudinal: longitudinal and paired-sample analyses of microbiome data. mSystems 3, doi:10.1128/mSystems.00219-18 (2018).

69. Quast C et al. The SILVA ribosomal RNA gene database project: improved data processing and web-based tools. Nucleic Acids Res 41, D590–596, doi:10.1093/nar/gks1219 (2013). [PubMed: 23193283]

70. Bray JR & Curtis JT An ordination of the upland forest communities of southern Wisconsin. Ecol. Monogr. 27, 325–349, doi:doi: 10.2307/1942268 (1957).

71. Bokulich NA et al. Optimizing taxonomic classification of marker-gene amplicon sequences with QIIME 2's q2-feature-classifier plugin. Microbiome 6, 90, doi:10.1186/s40168-018-0470-z (2018). [PubMed: 29773078]

72. Lozupone C & Knight R UniFrac: a new phylogenetic method for comparing microbial communities. Appl Environ Microbiol 71, 8228–8235, doi:71/12/8228 [pii] 10.1128/AEM.71.12.8228-8235.2005 (2005). [PubMed: 16332807]

73. Benjaminii Y & Hichberg Y Controlling the false discovery rate: a practical and powerful approach to multiple testing. J. R. Stat. Soc. Ser. B 57, 289–300, doi:doi: 10.1111/j.2517-6161.1995.tb02031.x (1995).

74. Afgan E et al. The Galaxy platform for accessible, reproducible and collaborative biomedical analyses: 2018 update. Nucleic Acids Res 46, W537–W544, doi:10.1093/nar/gky379 (2018). [PubMed: 29790989]

75. Segata N et al. Metagenomic biomarker discovery and explanation. Genome Biol 12, R60, doi:10.1186/gb-2011-12-6-r60 (2011). [PubMed: 21702898]

76. Mogavero S & Hube B *Candida albicans* interaction with oral epithelial cells: adhesion, invasion, and damage assays. Methods Mol Biol 2260, 133–143, doi:10.1007/978-1-0716-1182-1_9 (2021). [PubMed: 33405035]

77. Gerwien F et al. A novel hybrid iron regulation network combines features from pathogenic and nonpathogenic yeasts. mBio 7, doi:10.1128/mBio.01782-16 (2016).

78. Ramirez-Zavala B et al. The Snf1-activating kinase Sak1 is a key regulator of metabolic adaptation and *in vivo* fitness of *Candida albicans*. Mol Microbiol 104, 989–1007, doi:10.1111/mmi.13674 (2017). [PubMed: 28337802]

79. Miramon P et al. A family of glutathione peroxidases contributes to oxidative stress resistance in *Candida albicans*. Med Mycol 52, 223–239, doi:10.1093/mmy/myt021 (2014). [PubMed: 24625675]

80. Mallick H et al. Multivariable association discovery in population-scale meta-omics studies. PLoS Computational Biology 17, e1009442, doi:10.1371/journal.pcbi.1009442 (2021). [PubMed: 34784344]

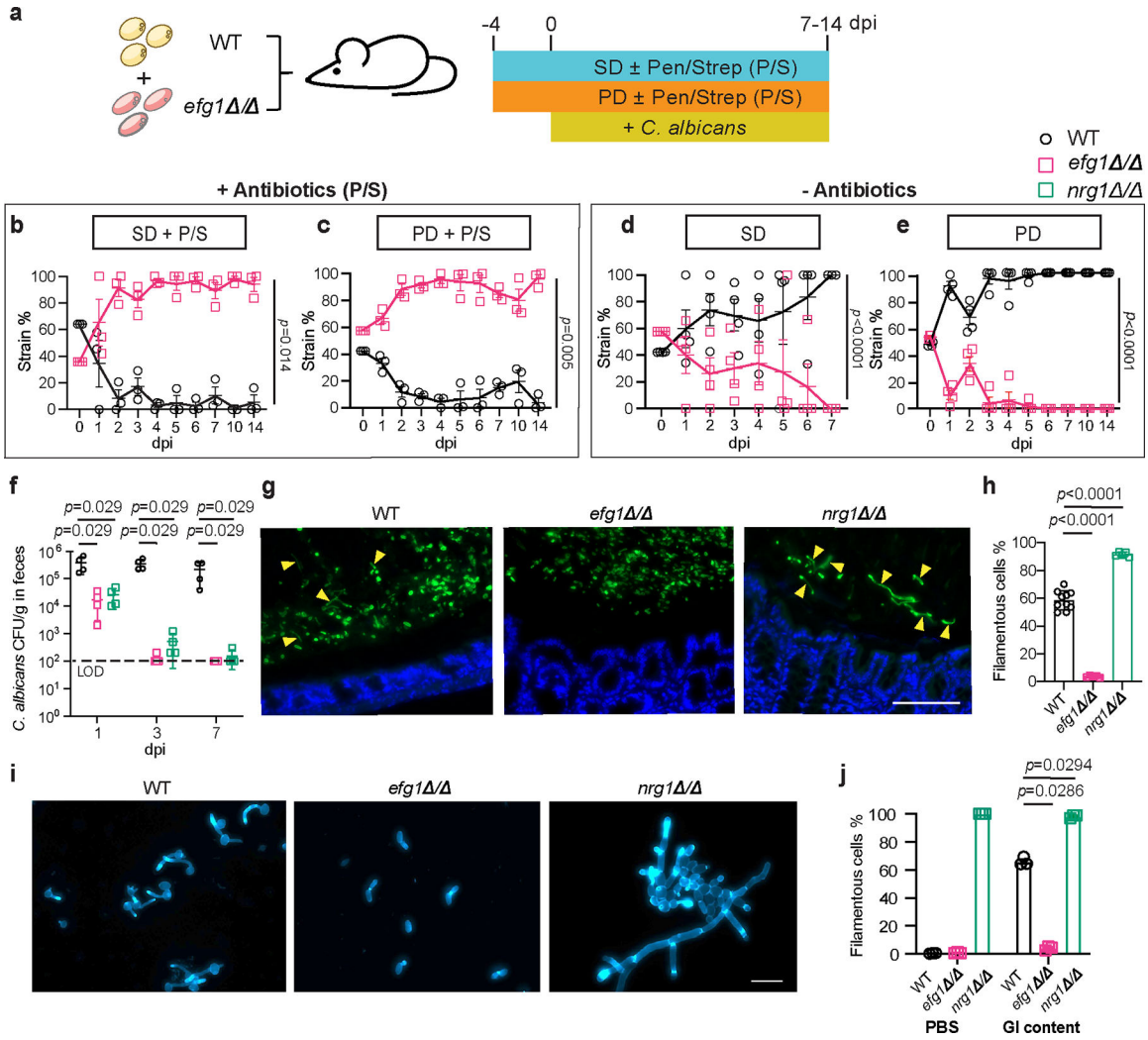

Fig. 1|. The colonization fitness of *C. albicans* WT and yeast-locked cells is dependent on the murine model.

a, Schematic of *C. albicans* colonization models. BALB/c mice were gavaged with a 1:1 mixture of WT and *efg1*Δ/Δ cells (or *EFG1*/*efg1Δ* and *efg1Δ/Δ* cells) while fed a standard diet (SD) or a purified diet (PD). Drinking water was supplemented with antibiotics (P/S; penicillin/streptomycin) as indicated. *C. albicans* colonies were examined in fecal pellets at the indicated time points (dpi; days post inoculation). **b-e**, WT (CAY2698) versus *efg1Δ/Δ* (CAY11750) competition in SD+P/S model (**b**), PD+P/S model (**c**), or SD model (**d**). *EFG1/efg1Δ* (CAY7064) and *efg1Δ/Δ* (CAY7769) were competed in the PD model (**e**). **f**, PD-fed mice were colonized with *C. albicans* and colony forming units (CFUs)/g in fecal pellets were determined. LOD, limit of detection. $n = 4$. **g**, Analysis of cell morphology of WT SC5314, *efg1Δ/Δ* and *nrg1Δ/Δ* cells. *C. albicans* cells were stained with anti-Candida antibody (green), while epithelial cells were stained with DAPI (blue) in the SD+P/S model. Scale bar, 100 μm. **h**, Quantitative analysis of yeast and filamentous morphotypes from colonic sections (C57BL6 mice), SD+P/S model. For WT, $n = 10$; *efg1Δ/Δ*, $n = 5$; *nrg1Δ/Δ*, $n = 5$. WT, CAY2698; *efg1 Δ/Δ*, CAY10965; *nrg1Δ/Δ*, CAY1398. **i**, Analysis of cell morphology of WT SC5314, *efg1Δ/Δ* and *nrg1Δ/Δ* cells cultured at 37°C in cecal

contents from PD-fed BALB/c mice. Scale bar, 20 μm. **j**, Quantitative analysis of yeast and filamentous morphotypes in cecal contents in (**i**). $n = 3$. Data are presented as mean ± s.e.m, each data point represents an individual mouse. For **j,** each data point represents individual experiments. Paired t-test (two-tailed) in **b**-**e**; Mann-Whitney (two-tailed) test in **f**,**h** and **j**.

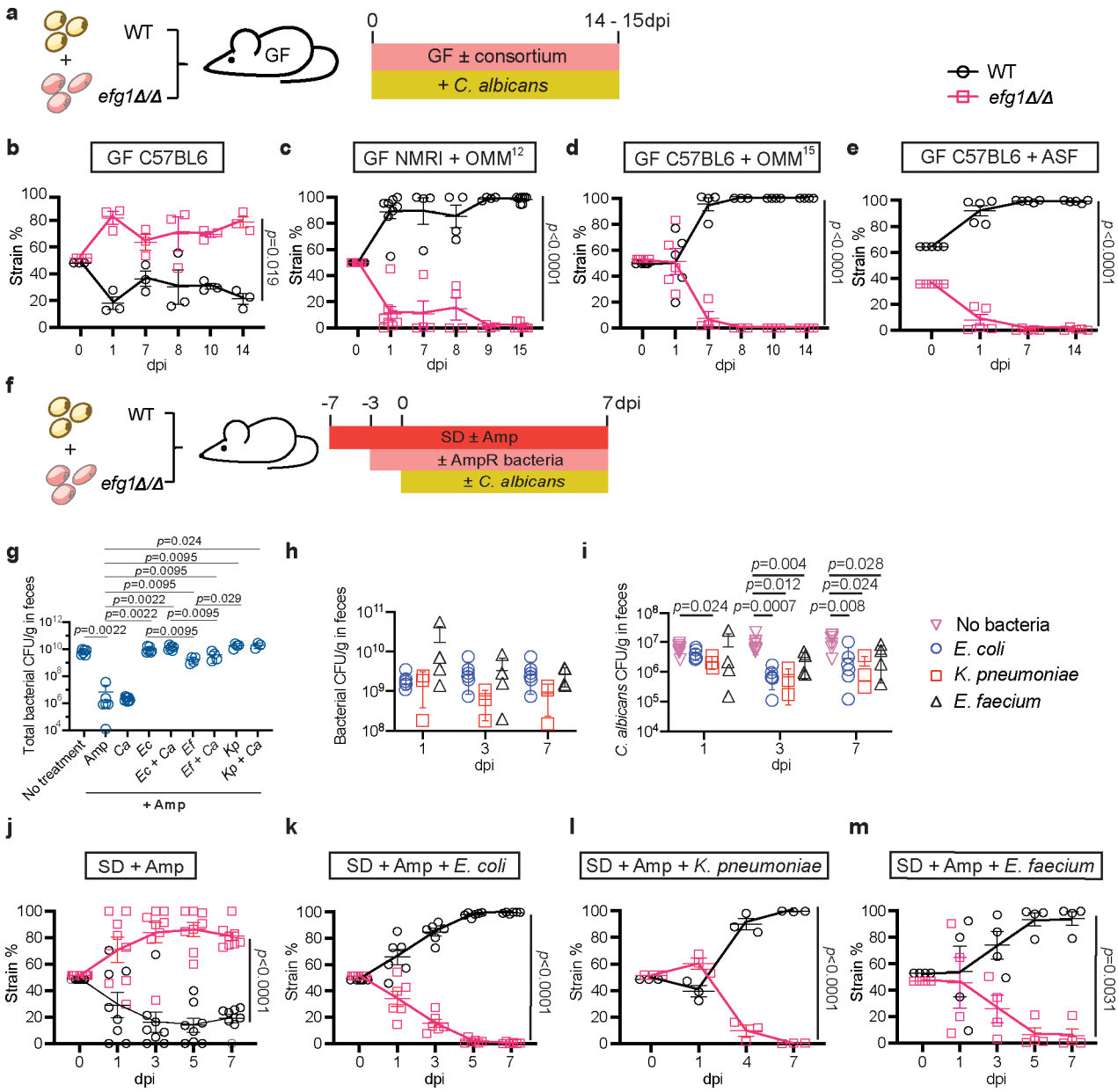

Fig. 2|. Colonization fitness of WT and yeast-locked *C. albicans* cells in hosts harboring different bacterial populations.

a, Schematic of gut colonization assays in gnotobiotic hosts that are germ-free (GF) or harbor different bacterial consortia. Mice were inoculated with a 1:1 mixture of WT and yeast-locked *efg1Δ/Δ* (CAY11750) cells (SC5314 background). **b-d**, Competition outcomes in GF C57BL/6 mice (**b**), NMRI mice harboring the Oligo-OMM12 consortium (**c**), C57BL/6 mice harboring the Oligo-OMM15 consortium (**d**), or those harboring the ASF consortium (**e**). **f**, Schematic of competition experiments using SD-fed mice supplemented with ampicillin (Amp). Mice were colonized with ampicillin-resistant (AmpR) bacteria prior to gavage with *C. albicans* or given *C. albicans* without bacteria. **g**, Total bacterial levels in fecal pellets were determined by quantitative PCR. No treatment; samples collected prior to Amp supplementation. *Ec*; *E. coli*, *Ef*; *E. faecium*, *Kp*; *K. pneumoniae*. **h**,**i**, Bacterial (**h**) and

C. albicans (**i**) CFUs were examined in fecal pellets at 1, 3, and 7 dpi. $n = 8$ in Amp-treated mice without bacteria, $n = 6$ in mice with *E. coli*, $n = 3$ in mice with *K. pneumoniae*, $n = 4$ in mice with *E. faecium*, and $n = 6$ in mice with no treatment. **j**, WT v. *efg1Δ/Δ* competition in Amp-treated mice. $n = 8$. **k-m**, Competitions performed in Amp-treated mice pre-colonized with AmpR *E. coli* (**k**), *K. pneumoniae* (**l**), or *E. faecium* (**m**). $n = 6$ in **k**, $n = 3$ in **l**, $n = 4$ in **m**. Each data point represents an individual mouse. Data are presented as mean ± s.e.m in **b-e** and **g-m**. A paired t-test (two-tailed) was used in **b-e** and **j-m** and Mann-Whitney (two-tailed) test in **g-i**.

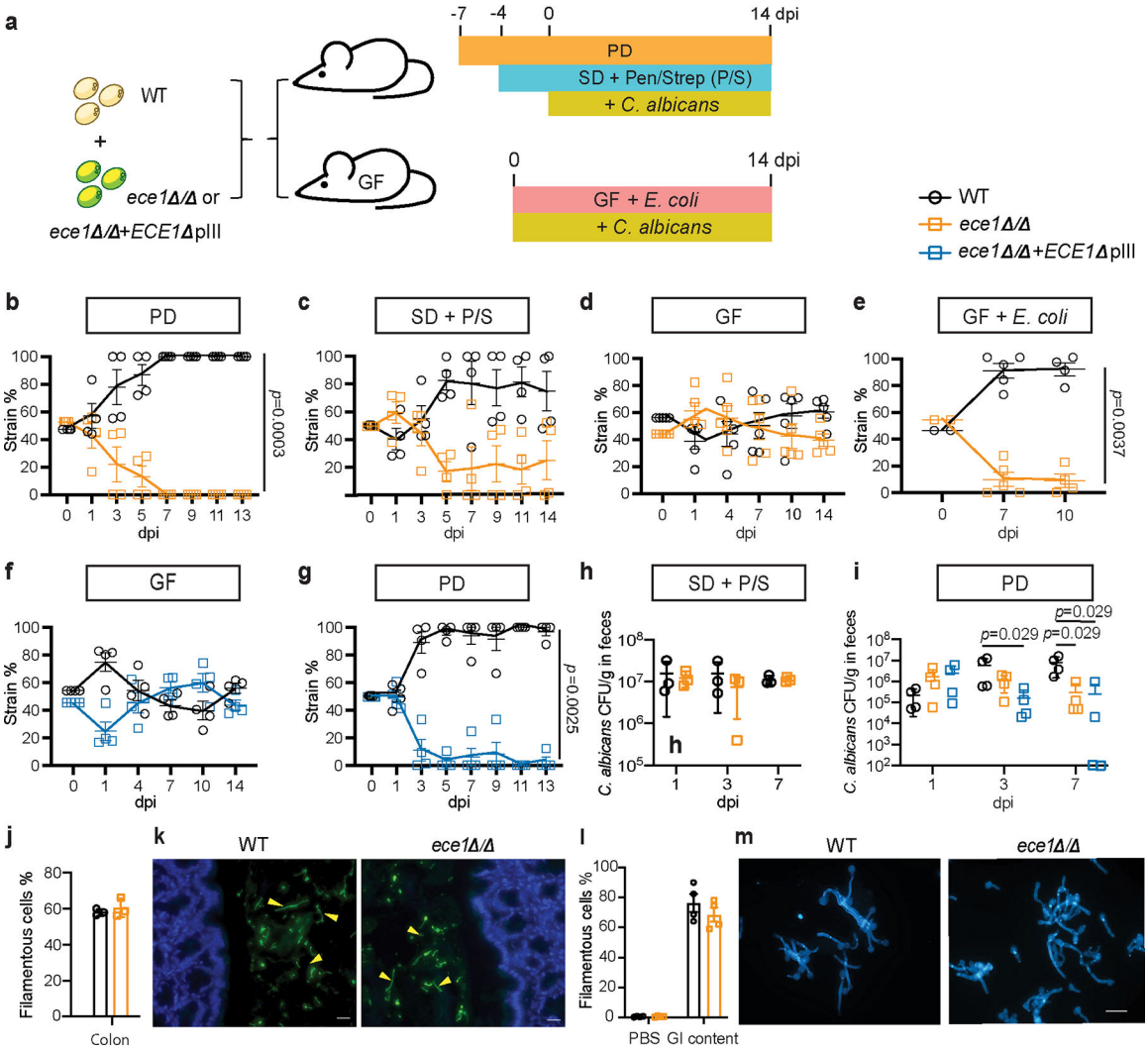

Fig. 3|. Candidalysin promotes *C. albicans* colonization in mice harboring intact (antibiotic-naïve) bacterial microbiomes.

a, Experimental design of *C. albicans* WT versus *ece1Δ/Δ* or *ece1Δ/Δ+ECE1ΔpIII* in conventional or gnotobiotic hosts. **b-e**, Competition between WT and *ece1Δ/Δ* cells in PD-fed BALB/c mice (**b**), SD-fed BALB/c mice on penicillin/streptomycin (P/S) antibiotics (**c**), GF C57BL/6 mice (**d**), and GF C57BL/6 mice pre-colonized with *E. coli* (**e**). WT (CAY12202) versus *ece1Δ/Δ* (CAY8578) in **b**, CAY11533 (WT) versus CAY11507 (*ece1Δ/Δ*) in **b**. $n = 4$ in **b**, $n = 5$ in **c**-**e**. **f,g**, Competitions between WT (CAY12202) and *ece1Δ/Δ+ECE1ΔpIII* (CAY8580) in GF C57BL/6 mice (**f**) and PD-fed BALB/c mice (**g**). $n = 4$. **h**, Colonization levels of WT (CAY2698) and *ece1Δ/Δ* (CAY8785) strains individually colonizing SD+P/S mice. $n = 3$. **i**, Colonization levels of WT (CAY2698), *ece1Δ/Δ* (CAY8785) and *ece1Δ/Δ+ECE1ΔpIII* (CAY8580) strains individually colonizing PD-fed mice. $n = 4$. **j**, **k**, Analysis of cells in the colon of BALB/c SD+P/S mice infected with WT (CAY2698) or *ece1Δ/Δ* (CAY8785) cells at 7 days post-infection. Percentage of filamentous cells (**j**). $n = 3$. Microscopic images (**k**). Hyphal cells indicated by arrows. Scale bar, 20 μm. **l**, **m**, Analysis of cell morphology of WT (CAY2698) and *ece1Δ/Δ* (CAY8785)

cells cultured at 37°C in cecal contents from PD-fed BALB/c mice, $n = 4$. Quantitative analysis of yeast and filamentous morphotypes (**l**). Microscopic images (**m**). Scale bar, 50 μm. Each data point represents an individual mouse. Data are presented as mean ± s.e.m for **b**-**j** and **l**. For **l,** each data point represents individual experiments. A paired t-test (two-tailed) was used in **b**-**g**, a Mann-Whitney (two-tailed) test in **h**, **i**, **j** and an unpaired t-test (two-tailed) in **l**.

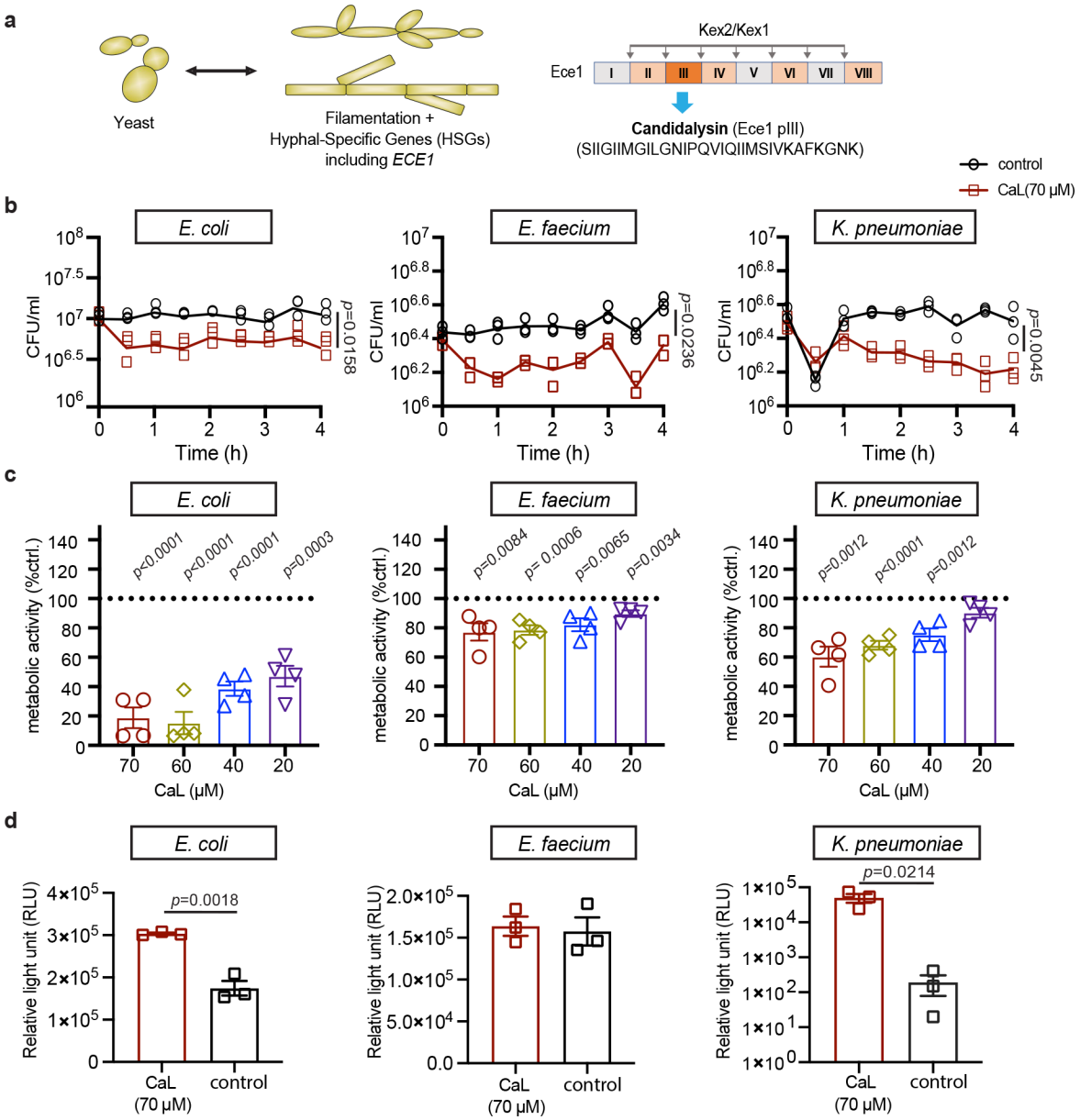

Fig. 4|. Candidalysin peptide exhibits direct antibacterial activity.

a, *C. albicans* can grow as yeast or filamentous forms including pseudophyphae or true hyphae. Hyphal cells express a set of hyphal-specific genes (HSGs) that include *ECE1* encoding the candidalysin toxin. The Ece1 proprotein is proteolytically processed by Kex2 and Kex1 to produce mature candidalysin peptide (CaL). **b**, Analysis of *E. coli*, *E. faecium*, and *K. pneumoniae* colony forming units (CFUs) when challenged with 70 μM CaL in PBS at 37°C for the indicated times. $n = 3$. **c**, Effect of candidalysin on bacterial metabolism as determined by XTT assays. Activity is shown as a ratio of the no candidalysin control (dotted line), $n = 4$. **d**, Effect of different concentrations of candidalysin on glucose uptake, $n = 3$. Data are presented as mean ± s.e.m, each data point represents individual independent experiments. An unpaired t-test (two-tailed) was used to determine significance (**b**-**d**).